CHEMICAL ENGINEERING
January 2020
ESSENTIALS FOR THE CPI PROFESSIONAL
www.chemengonline.com

Evaporators

Sampling System Design

Particle Size

SIL Misconceptions

Facts at Your Fingertips: Particulate Matter

Focus on Motor and Drives

Production of Nitrobenzene

Achievements in Chemical Engineering

page 23

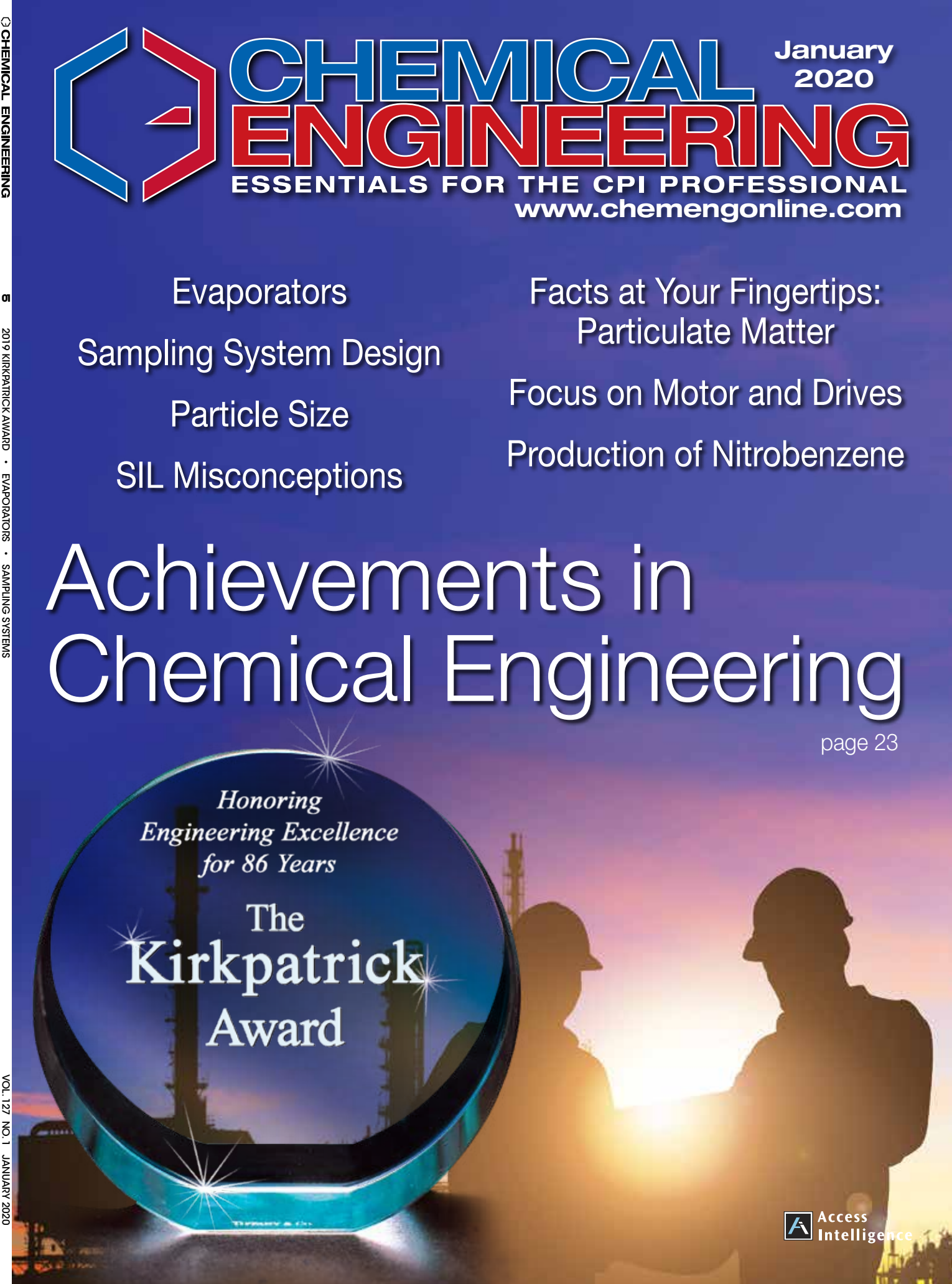

Access Intelligence

CHEMICAL ENGINEERING
ESSENTIALS FOR THE CPI PROFESSIONAL
www.chemengonline.com

January 2020 Volume 127 | no. 1

Cover Story

23

In the News

12

Technical and Practical

39

16

18

Equipment and Services

Departments

Advertisers

Chemical Connections

Follow @ChemEngMag on Twitter

Join the *Chemical Engineering* Magazine LinkedIn Group

Visit us on www.chemengonline.com for more articles, Latest News, Webinars, Test your Knowledge Quizzes, Bookshelf and more

Coming in February

Look for: **Feature Reports** on Cybersecurity; and Process Safety; A **Focus** on Sensors; A **Facts at your Fingertips** on Solids Separation; **News Articles** on Catalytic Cracking Technology; and Pumps; **New Products**; and much more

Cover design: Rob Hudgins

CHEMICAL ENGINEERING
ESSENTIALS FOR THE CPI PROFESSIONAL

HEADQUARTERS

40 Wall Street, 50th floor, New York, NY 10005, U.S.
Tel: 212-621-4900
Fax: 212-621-4694

EUROPEAN EDITORIAL OFFICES

Zeilweg 44, D-60439 Frankfurt am Main, Germany
Tel: 49-69-9573-8296
Fax: 49-69-5700-2484

CIRCULATION REQUESTS:

Tel: 800-777-5006
Fax: 301-309-3847
Chemical Engineering, 9211 Corporate Blvd.,
4th Floor, Rockville, MD 20850
email: clientservices@accessintel.com

ADVERTISING REQUESTS: SEE P. 50

ACCESS INTELLIGENCE, LLC

DON PAZOUR
Chief Executive Officer

HEATHER FARLEY
Chief Operating Officer

JAMES OGLE
Executive Vice President
& Chief Financial Officer

MACY L. FECTO
Chief People Officer

JENNIFER SCHWARTZ
Senior Vice President & Group Publisher
Aerospace, Energy, Healthcare

ROB PACIOREK
Senior Vice President,
Chief Information Officer

JONATHAN RAY
Vice President, Digital

MICHAEL KRAUS
Vice President,
Production, Digital Media & Design

GERALD STASKO
Vice President/Corporate Controller

Access Intelligence
9211 Corporate Blvd., 4th Floor
Rockville, MD 20850-3240
www.accessintel.com

BPA

Editor's Page

CPI outlook slower, but positive

Despite a slowdown in global manufacturing, the U.S. chemical process industries (CPI) have continued to expand and remain a positive contributor to growth. In its "Year-End 2019 Chemical Industry Situation and Outlook," which was issued in December, the American Chemistry Council (ACC; www.americanchemistry.com) says that "With a weaker outlook for the U.S. industrial sector, slow growth in key trading partner economies, new tariff burdens and unprecedented uncertainty related to U.S. trade policy, the chemical industry is one of few manufacturing segments expected to grow over the next year."

The upside: energy costs

As the largest energy-consuming manufacturing sector in the U.S., the CPI have been benefitting from the abundance of domestic natural gas. And the affordable, natural gas supply has driven global CPI investments in the U.S. According to the ACC, about 340 new chemical production projects at a total value of approximately $204 billion have been announced in the past decade, with 70% of them including either foreign direct investment or foreign partners.

Examples of recent announcements include one made in June by ExxonMobil and SABIC. The two companies are moving forward with construction of a 1.8-million-metric-ton ethane steam cracker, two polyethylene units and a monoethylene glycol unit in Texas. The project is a 50/50 joint-venture between ExxonMobil and SABIC called Gulf Coast Growth Ventures (www.gulfcoastgv.com). Startup is anticipated by 2022. Estimates indicate over $22 billion in economic output during construction.

In another announcement made in July of this year, Chevron Phillips Chemical Co. and Qatar Petroleum agreed to jointly pursue a new petrochemical plant in the Gulf Coast region to include an ethylene cracker and two high-density polyethylene units. The cost would be $8 billion. A final decision on the proposed plant is expected in 2021 with possible startup in 2024.

The ACC anticipates that over the next five years, most of the growth in the U.S. will occur in the Gulf Coast region, followed by the Midwest and Ohio Valley regions. Petrochemicals, organic intermediates and plastic resins are expected to bring the most capital spending, for example for process equipment, instrumentation and structures.

The downside: trade tensions

While the outlook for the CPI is positive, much depends on global trade policies, which have been volatile, particularly in recent months. According to the ACC report, increasing trade tensions in the second half of 2019 resulted in decreased expectations for chemicals trade growth. The report states that "With resolution of the trade tensions, uncertainty will be alleviated and prospects should improve during 2020, with global chemicals output rising 2.0% and 2.7% in 2020 and 2021, respectively."

Trends

The CPI continue to look for ways to increase efficiencies by reducing waste, and through more efficient use of raw materials and energy. Technologies and policies related to sustainability and climate change issues are garnering much interest. We look forward to continuing to cover these and many more advances in the CPI for our readers this year. Best wishes to all for 2020.

Dorothy Lozowski, Editorial Director

Bottom-up synthesis of new perovskite material for ammonia production

Perovskites are a class of synthetic materials that have a crystalline structure similar to that of the naturally occurring mineral calcium titanate. They have been the subject of many studies because they exhibit unique properties that can be tuned according to their composition. One of their potential applications is as catalysts for the synthesis of ammonia. For example, recently, perovskites with some of their oxygen atoms replaced by hydrogen and nitrogen ions have been developed as efficient catalysts for ammonia synthesis. However, the traditional synthesis of perovskites with such substitutions usually has to be carried out at high temperatures (more than 800°C) and over long periods of time (weeks).

To address these issues, in a recent study carried out at Tokyo Institute of Technology (TiTech; Yokohama Campus, Japan; www.titech.ac.jp), a group of researchers led by professor Masaaki Kitano devised a novel method for the low-temperature synthesis of one such oxygen-substituted perovskite with the general formula $BaCeO_{3-x}N_yH_z$ (diagram) and tested its performance as a catalyst to produce ammonia. To achieve this, they made an innovative alteration to the perovskite synthesis process. The use of barium carbonate and cerium dioxide as precursors involves a very high temperature that would be required to have them combine into the base perovskite, or $BaCeO_3$, because barium carbonate is very stable. In addition, one would then have to substitute the oxygen atoms with nitrogen and hydrogen ions. On the other hand, the team found that the compound barium amide reacts easily with cerium dioxide under ammonia gas flow to directly form $BaCeO_{3-x}N_yH_z$ at low temperatures (300–600°C) and in less time (6 h). "This is the first demonstration of a bottom-up synthesis of such a material, referred to as perovskite-type oxynitride-hydride," says Kitano. "Our results will pave the way in new catalyst design strategies for low-temperature ammonia synthesis."

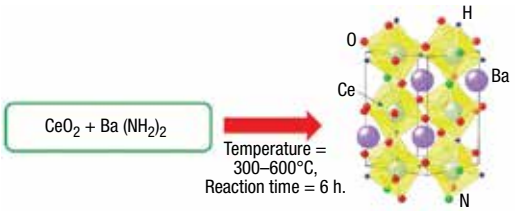

Tokyo Institute of Technology

Metals from nodules on seabed offer environmental advantages

Small-scale pilot testing has begun for a process that extracts nickel, manganese, cobalt and copper from nodules collected from the surface of the Pacific Ocean seafloor. Obtaining the metals from the seabed nodules has advantages over mining land-based ores because the nodules contain far less toxic heavy metals and can be processed with zero tailings, according to process developer DeepGreen Metals Inc. (Vancouver, B.C.; www.deep.green).

The nodules are formed on the seafloor four to six km deep in the Clarion-Clipperton Zone, a region of the Pacific Ocean between Hawaii and Mexico where the conditions permit precipitation of metal compounds onto nuclei of silica or calcium carbonate particles. The nodules contain around 30% Mn, 1.38% Ni, 1.17% Cu, 0.13% Co, and small amounts of zinc and rare-earth elements, explains Jeff Donald, head of onshore development at DeepGreen. Using robotic technology inspired by the undersea-cable-laying industry, DeepGreen harvests the nodules from the seafloor and raises them for further processing.

"The nodules contain metals in combinations that don't exist in typical ore bodies on land . . . "So we had to adapt existing metallurgical processes in novel ways to extract and refine the nodule metals." Using methodology from the nickel industry, DeepGreen devised a specialized pyrometallurgical process of calcining and smelting that is designed to obtain the desired metal compounds. This is followed by a series of refining steps using leaching and hydrometallurgy techniques. "The only real waste stream from the process is an iron-rich slag that can be used as aggregate for road building," Donald says, so the nodules are fully utilized.

Ni and Co are obtained as battery-grade sulfates that can be used in batteries for electric vehicles, while the Mn can be used for alloying steel, and Cu as wiring. Donald says the company is currently working with the International Seabed Authority on environmental impact studies and continuing pilot testing for the on-shore process.

Edited by:
Gerald Ondrey

SLUDGE TO FUEL

Bio-sludge is a byproduct of the wastewater treatment process at Stora Enso Oy's (Helsinki, Finland; www.storaenso.com) Heinola fluting mill in Finland. In the past, the mill had been burning the bio-sludge at the power station for generating thermal power, but this required additional fossil-based fuels to support the combustion due to the large water content of the sludge. In an effort to meet the mill's long-term goal to achieve carbon neutrality in production, the company started up (in 2019) an industrial-scale pilot plant that dries the wet bio-sludge in an energy-efficient way, using pressure and heat, into a solid fuel. The plant uses a process developed and patented by C-Green Technology AB (Solna, Sweden; www.c-green.se). "Our process, OxyPower HTC, uses an innovative application of hydrothermal carbonization, which converts complex organic compounds into sterile odorless biofuel," says Erik Odén, CEO of C-Green.

The pilot plant processes 16,000 metric tons of biowaste per year. The resulting biofuel is used in the mill's power boiler and to heat the nearby town of Heinola, with about 20,000 inhabitants. Heinola Mill has been providing district heat to the city and its residents since the 1980s.

RECYCLING NADH

The Center for Process Innovation, Ltd. (CPI; Wilton, U.K.; www.uk-cpi.com) has collaborated with professor Kylie Vincent and colleague Holly Reeve at the University of Oxford (U.K.; www.chem.ox.ac.uk) to support the scale-up of HydRegen,

(Continues on p. 6)

a technology for recycling nicotinamide adenine dinucleotide (NAD+/NADH). NADH is a critical but very expensive cofactor of many biocatalytic reactions.

Biocatalysis provides safer and more sustainable chemical processing by using enzymes in place of metal-based catalysts (which are often toxic) and replacing flammable organic solvents with water. Scaling up production of HydRegen will allow the University of Oxford to evaluate the technology in an industrial setting.

HydRegen immobilizes enzymes from the bacterium *Cupriavidus necator* onto carbon beads. In the presence of H_2 gas, these enzymes readily recycle the NADH consumed in the reaction, creating a much more efficient biocatalytic platform. The immobilized enzymes are easily recovered from the final product, ultimately leading to a more sustainable and cost-effective process.

Initially, CPI has worked to adapt Oxford's bacterial growth protocol in order to attain the biomass concentration needed for large-scale production of the enzymes. CPI's extensive experience in scaling up biotechnologies at the National Industrial Biotechnology Facility enabled them to successfully achieve a 10-fold higher biomass than previously reported. Further work aims to increase the yield of enzymes harnessed from these cultures.

CO TO ETHYLENE

Today, most routes to ethylene are based on fossil-fuel feedstocks, and require high temperatures, such as the steam cracking of naphtha at 800–900°C, or the Fischer-Tropsch (F-T) conversion of coal-gasification-derived synthesis gas at 200–450°C and 5–50 bars pressure. Besides generating considerable CO_2 emissions, both of these routes also have a relatively low selectivity for ethylene,

(Continues on p. 7)

New material promises to enhance performance of gas-separation membranes

Toray Industries

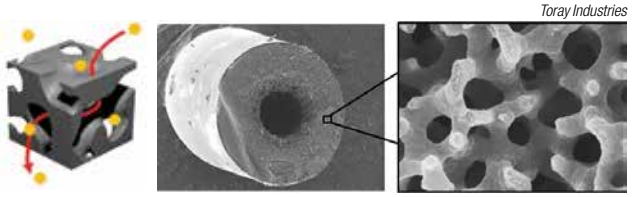

Harnessing its polymer technology and carbon-fiber expertise has enabled Toray Industries, Inc. (Tokyo, Japan; www.toray.com) to create a porous carbon fiber with uniformly continuous pores (diagram) — claimed to be a world's first. Using this fiber as a support layer could reduce the weight of advanced membranes used for gas separation and make them more compact, thereby enhancing performance, says the company.

The sizes for the pore structure can be adjusted from the nanometer to micrometer scale. It is also possible to create a hollow fiber-shaped porous carbon fiber in the center of a fiber. The new material is said to have "outstanding" gas permeability, and excellent adsorption capacity, making it suitable for gas separation, as well as for electrode materials and catalyst supports for advanced batteries.

Last month, Toray opened its R&D Innovation Center for the Future on the premises of the Shiga Plant, where the company started out in 1926. The new facility will serve as a global headquarters for strategic innovations by engaging with academic institutions and key partners from diverse fields. The company will collaborate with several partners in efforts leveraging its new material in a drive to commercialize more advanced gas-separation membranes for applications such as natural gas and biogas purification and hydrogen production.

A Pt-free electrode promises to cut costs for fuel cells and metal-air batteries

Hiroya Abe and colleagues at Tohoku University (Sendai, www.tohoku.ac.jp) and Hokkaido University have developed a method to fabricate a highly active catalyst electrode for performing the oxygen reduction reaction (ORR) in fuel cells and metal-air batteries. Currently, such fuel cells and metal-air batteries need expensive platinum-based carbon (Pt/C) electrodes for the reaction.

The research group has designed a new class of Pt-free catalysts that included molecular iron phthalocyanine (FePc) derivatives, namely, iron azaphthalocyanine (FeAzPc) unimolecular layers (Fe AzULs) adsorbed on oxidized multiwall carbon nanotubes (oxMWCNTs). FeAzPcs were dissolved in organic solvents such as dimethyl sulfoxide (DMSO), and catalytic electrodes modified with molecularly adsorbed FeAzPcs were successfully prepared. The optimized composition of the catalytic electrodes was determined, and the electrodes exhibited superior activity for the ORR, as well as being more durable than conventional FePc catalytic electrodes and commercial Pt/C. The catalytic electrodes that were molecularly modified with FeAzPcs have higher activities than those composed of FeAzPc crystals and oxMWCNTs. Unlike other Pt-free catalytic electrodes, the Fe AzUL catalytic electrodes can be prepared by low-cost processing without pyrolysis and are therefore promising catalytic electrode materials for applications, such as polymer electrolyte fuel cells and metal-air batteries.

A spin-off company, Azul Energy Co., Ltd., was established last July to commercialize the technology.

Non-halogenated flame-retardant material

Dynamic Modifiers LLC (Atlanta, Ga.; www.dynamicmodifiers.com), a maker of custom polyolefin compounds, recently introduced PAL…VersaCHAR, a non-halogenated flame-retardant polymer designed to be molded over other materials. When exposed to flame, the formulation's surface chars quickly, which prevents flame spread and rapidly self-extinguishes, the company says. PAL…VersaCHAR can be made into flexible films and sheets, or can be made to coat fabric, protecting the underlying substrate in the event of flame exposure. The company says the material has been successfully tested at up to 1,950°C with no flaming polymer drips. The material is free of heavy metals, halogens and volatile organic compounds, says Dynamic Modifiers, and is designed for demanding industrial and commercial applications.

Cascade reactions on 'nanozymes' make chemicals from CO_2

An international team of researchers has developed metallic nanoparticles that imitate enzymes to convert carbon dioxide into ethanol and propanol, which are common raw materials for the chemical industry. The team includes professors Justin Gooding and Richard Tilley from the University of New South Wales (Sydney, Australia; www.unsw.edu.au), professor Wolfgang Schuhmann from Ruhr-Universität Bochum (Bochum, Germany; www.ruhr-uni-bochum.de), and professor Corina Andronescu from Universität Duisburg-Essen (Duisburg, Germany; www.uni-due.de).

The team adopted the principle from enzymes that produce complex molecules in multi-step reactions. It transferred this mechanism to metallic nanoparticles, also known as nanozymes. A single enzyme can generate a complex product from a simple starting material. To imitate this, the team synthesized a particle with a silver core surrounded by a porous layer of copper. The silver core is the first active center, the copper layer is the second. Intermediate products formed at the silver core then react in the copper layer to form more complex molecules, which eventually leave the particle.

The team showed that the electrochemical reduction of CO_2 can take place with the help of nanozymes. Several reaction steps on the silver core and copper shell transform the starting material into ethanol and propanol.

Schuhmann says transferring the cascade reactions of the enzymes to catalytically active nanoparticles could be a decisive step in the design of new catalysts. There are other nanoparticles that can produce ethanol and propanol from CO_2 without the cascade principle, but they require considerably more energy.

The team aims to further develop the concept of the cascade reaction in nanoparticles to produce molecules such as ethylene and butanol.

generating at best a maximum of 30% of C2 products, which must then be separated from other byproducts.

Researchers working with professor Dehui Deng at Xiamen University (https://en.xmu.edu.cn) and the Dalian Institute of Chemical Physics of the Chinese Academy of Sciences (http://english.dicp.cas.cn) have now introduced a new approach for a direct electrocatalytic process for the highly selective production of ethylene. In this method, CO is reduced with water at room temperature and standard pressure, using a copper catalyst and electric current.

By optimizing the structure of their gas-diffusion electrode, the researchers were able to achieve an unmatched Faradaic efficiency (charge-transfer efficiency within an electrochemical reaction) of 52.7%. Based on CO conversion to

(Continues on p. 8)

ethylene, a selectivity of around 70% was observed, which is much higher than the 30% obtained by F-T synthesis, and no CO_2 emission occurs.

The success of the approach, as described in a recent issue of *Angewandte Chemie Int. Ed.*, hinges on a microporous layer of carbon fibers with an optimally tuned hydrophobicity, which acts as a support for catalytically active Cu particles, and an optimized KOH concentration in the aqueous phase. This increases the CO concentration at the electrode and increases coupling between the carbon atoms. The side products (ethanol, *n*-propanol, and acetic acid) are liquids, which are easy to separate from gaseous ethylene.

DIGESTATE UTILIZATION

A new E.U.-funded project aims to build a production plant on a truck to give every farmer the opportunity to easily access natural fertilizers. For this, the researchers of the Nomad Project (Novel Organic recovery using Mobile ADvanced technology) want to use fermentation residue (digestate), a byproduct of energy production in biogas plants.

European and Chinese partners of the Nomad project will develop a decentralized model that aims to deliver a complete, localized, circular solution for digestate use. The plan is to build a prototype plant for this transformation process and integrate it onto a trailer for easy transport by road. Once the prototype has been built and tested in the U.K., the trailer will be moved to Greece, Italy and Malta to be applied at different demonstration sites with very different types of organic waste (U.K.: food waste; Greece: animal residue and manure; Italy: crop waste; Malta: municipal wastewater). This approach should enable farmers not only in remote areas, but also eventually in urban areas, to convert their unused organic residues into high performance bio-fertilizer.

Another key aim of the research team is to address the problem of antibiotic residues that end up in digestate derived from manure and slurries. A new technology being developed as part of the project will remove dangerous pharmaceutical compounds from the digestate.

(Continues on p. 9)

A new method to study nanoparticles

Researchers from the Singapore-MIT Alliance for Research and Technology (Singapore; https://smart.mit.edu) have discovered a way to study the properties of a nanoparticle without damaging it, which has not been possible so far. The work was led by Michael Strano, a professor at MIT (Cambridge, Mass.; www.mit.edu), and a principal investigator of DiSTAP — the Disruptive & Sustainable Technologies for Agricultural Precision Interdisciplinary Research Group — which is a part of Smart. DiSTAP develops new technologies to enable Singapore to improve its agriculture yield to reduce its dependence on imported food and produce.

The researchers' method, called molecular probe adsorption (MPA), is based on a non-invasive adsorption of a fluorescent probe on the surface of colloidal nanoparticles in aqueous phase.

The corona phase — the adsorbed layer of polymer, surfactant, or stabilizer molecules around a nanoparticle — is typically used to disperse nanoparticles into a solution or solid phase. However, this phase also controls molecular access to the nanoparticle surface. The MPA method allows measuring the accessible nanoparticle surface using a titration of a quenchable fluorescent molecule.

A material balance on the titration yields certain surface coverage parameters, including the ratio of the surface area (q) to the dissociation constant (K_d) of the fluorophore, q/K_d, as well as K_d itself. Using MPA across a series of corona phases, the researchers found that the Gibbs free energy of probe binding scales inversely with the cubic root of the surface area, q.

The researchers say MPA is the only technique to date capable of discerning critical structure-property relationships for such nanoparticle surface phases. They say the MPA method is also able to characterize a nanoparticle within minutes compared with several hours that the best chemical methods require today. Because it uses only fluorescent light, the MPA method is also substantially cheaper than other methods.

DiSTAP is using the MPA method for nanoparticle sensors in plants and nanocarriers for delivery of molecular cargo into plants. Strano says with better data and insight into plant biochemistry, we can provide optimal nutrient levels for healthier plants and higher yields.

Waste garlic stems make an adsorbent for arsenic removal

Professor Monoj Kumar Mondal and Anuj Kumar Prajapati from the Dept. of Chemical Engineering and Technology, Indian Institute of Technology (Banaras Hindu University, Varanasi, India; www.iitbhu.ac.in) have used nanoporous activated garlic stem carbon (AGSC) — prepared from garlic stem waste — to remove arsenide ions [As(III)], from synthetic water samples and from groundwater.

They performed batch adsorption experiments to study the adsorption of As(III) onto AGSC. They obtained maximum removal of 93.3% of As(III) at optimum condition pH = 6, adsorbent dose of 5 g/L, equilibrium time of 150 min, initial As(III) concentration 400 µg/L, and temperature 298K. The maximum adsorption capacity of AGSC for As(III) removal was found to be 192.30 µg/g. The adsorption process of As(III) onto AGSC was shown to be both exothermic and spontaneous.

Arsenic is one of the most toxic metalloids present in groundwater and other water bodies. It is found in various oxidation states, but is mostly found in tri- and pentavalent form. The U.S. Environmental Protection Agency (Washington, D.C.; www.epa.gov) and the World Health Organization (WHO; Geneva, Switzerland; www.who.int) have set the maximum allowable level for total arsenic in water for human use at 10 µg/L. Several technologies have been used to keep the concentration of arsenic in water below 10 µg/L, however these technologies often involve high process cost, low removal efficiency and toxic reagents. Adsorption can be economical if the adsorbent is prepared from abundantly available waste materials, is of inexpensive preparation, and exhibits good regeneration ability.

India is the world's second largest producer of garlic. Garlic stem is a waste burned by farmers. This decreases air quality, and is one of the reasons why the authors of this study chose the waste garlic stem for producing active carbon.

Integrated AC process eliminates refrigerants

With the goal of decreasing the climate impact of residential air conditioning (AC), Kraton Corp. (Houston; www.kraton.com) has developed the NexarCool technology in collaboration with Texas A&M University (College Station; www.tamu.edu), India Institute of Technology Bombay (www.iitb.ac.in) and Indian companies Porus Laboratories Ltd. and Infosys Ltd. "NexarCool is a novel water-based space-cooling technology that is free of the chemical refrigerants commonly used in standard AC, which are a significant source of ozone depletion and global warming," explains Vijay Mhetar, senior vice president and chief technology officer of Kraton. Leveraging the moisture-transport properties of Kraton's Nexar copolymer, the technology can effectively control humidity and temperature independently, since it contains a water-based evaporative cooler and an electro-osmotic membrane dehumidifier unit that work in tandem, says Mhetar. Furthermore, the technology does not require a compressor, which further improves upon its energy efficiency. In the NexarCool system, water vapor from indoor air is ejected to the outside when voltage is applied to the membrane dehumidifier unit. The dry indoor air is then passed to the evaporative cooling segment, where it is cooled as it loses heat to evaporate the water.

NexarCool has been demonstrated at laboratory scale, and the partners are working toward a fully integrated prototype unit and scaling up critical components of the value chain to reduce the cost per unit. The prototype will be tested in a laboratory that simulates the climates of different Indian cities. Since the technology is targeted for residential applications, the cost is key, emphasizes Mhetar. "The greatest needs for innovative cooling technologies are often in emerging markets. Therefore, affordability is considered a key barrier to scale," he adds. Beyond residential AC, Kraton is exploring potential applications in humidification, dehumidification and atmospheric water harvesting. ■

LNG PRETREATMENT

All over the world, but especially along the U.S. Gulf Coast, liquefied natural gas (LNG) production plants operating on lean natural-gas feeds struggle to remove traces of benzene, toluene and xylenes (BTX) and hydrocarbons, which cause freezing in the cold box and results in plant downtime. The mechanical solutions to this challenge can be costly and can require external solvent and increases plant complexity, according to BASF SE (Ludwigshafen, Germany; www.basf.com).

To address this problem, BASF added Durasorb HRU to its Durasorb portfolio of products for LNG pretreatment. Durasorb HRU is designed to remove BTX and heavy hydrocarbons. It provides a 30% increase in capacity for BTX components, allowing for the effective removal of BTX to less than 1 part per million (ppm) without compromising unit efficiency, says BASF. ❐

LINEUP

AGILYX
ARCHROMA
ARZEDA
BASF
BP
DUPONT
EVONIK
HALDOR TOPSOE
HUNTSMAN
INDORAMA
INEOS STYROLUTION
LANXESS
MCDERMOTT
MESSER
MITSUBISHI CHEMICAL
MOL GROUP
NEXT WAVE ENERGY
SASOL
SOLVAY
THYSSENKRUPP INDUSTRIAL SOLUTIONS
UMICORE

Look for more latest news on chemengonline.com

Plant Watch

Messer to build onsite gas facility for MOL polyols plant in Hungary

December 12, 2019 — Messer Group GmbH (Bad Soden, Germany; www.messergroup.com) will construct a new onsite gas facility for MOL Group (Budapest, Hungary; www.molgroup.info) in Tiszaújváros, Hungary. The plant will supply nitrogen and instrument air for MOL's new polyols complex, which is due to begin operations in 2021. With approximately 14,500 m^3/h of nitrogen and 27,000 m^3/h of instrument air, this plant will be one of Messer's largest onsite facilities in southeast Europe.

Serba Dinamik taps thyssenkrupp to build modular chlorine plant in Uzbekistan

December 12, 2019 — Thyssenkrupp Industrial Solutions AG (Essen, Germany; www.thyssenkrupp-industrial-solutions.com) has secured a contract with Serba Dinamik International for the engineering and procurement of a new modular chlor-alkali plant. The greenfield plant, which will have a processing capacity of 90 tons/d of chlorine, will be built in the Hazarasp Free Economic Zone in Uzbekistan. The new plant will produce caustic soda flakes, liquid chlorine and sodium hypochlorite. The plant's startup is planned for the second quarter of 2022.

McDermott awarded contract for Next Wave alkylate production facility

December 12, 2019 — McDermott International, Inc. (Houston; www.mcdermott.com) was awarded a technology contract for Next Wave Energy Partners' (Houston; www.nextwaveenergy.com) grassroots alkylate production facility in Pasadena, Tex. The new alkylate site will have a nameplate capacity of 28,000 barrels per day (bbl/d). Next Wave expects production to commence by mid-2022.

Ineos Styrolution and Agilyx planning a polystyrene-recycling plant in Illinois

December 9, 2019 — Ineos Styrolution (Frankfurt, Germany; www.ineos-styrolution.com) and Agilyx (Tigard, Ore.; www.agilyx.com) are advancing the development of a polystyrene chemical-recycling facility in Channahon, Ill. The facility will be capable of processing up to 100 ton/d of post-consumer polystyrene and converting it into a styrene product that will go into the manufacture of new polystyrene products.

Evonik to increase sodium methylate production capacity in Argentina

December 3, 2019 — Evonik Industries AG (Essen, Germany; www.evonik.com) plans to increase its capacity for sodium methylate at its Rosario/Santa Fe facility in Argentina from 60,000 metric tons per year (m.t./yr) up to 90,000 m.t./yr. The expansion is driven by growing demand for biodiesel in South America. Sodium methylate is an important catalyst for large-scale biodiesel production.

Solvay to double capacity at Changshu PVDF plant

November 26, 2019 — Solvay S.A. (Brussels, Belgium; www.solvay.com) is more than doubling its production capacity of high-performance, polymer-grade polyvinylidene fluoride (PVDF) at its production site in Changshu, China. The expansion is driven by growth demand for PVDF in applications in lithium-ion batteries for electric vehicles.

BASF commences its smart Verbund project in Zhanjiang, China

November 24, 2019 — BASF SE (Ludwigshafen, Germany; www.basf.com) has launched its smart Verbund project in Zhanjiang, China, and commenced building its first plants. It marks a milestone of the company's $10-billion investment project. The first plants will produce engineering plastics and thermoplastic polyurethane (TPU). By 2022, the new engineering-plastics compounding plant will supply an additional capacity of 60,000 m.t./yr in China, bringing BASF's total capacity of these products in the Asia Pacific region to 290,000 m.t./yr.

Mergers & Acquisitions

DuPont to acquire RO specialist Desalitech

December 11, 2019 — DuPont (Wilmington, Del.; www.dupont.com) signed an agreement to acquire Desalitech Ltd. (Boston, Mass.; www.desalitech.com), a closed-circuit reverse osmosis (CCRO) company. Desalitech's patented technology has been deployed at more than 200 sites over the past seven years.

BP and Arzeda enter second phase of renewable chemicals collaboration

December 11, 2019 — BP plc (London; www.bp.com) and Arzeda (Seattle, Wash.; www.azeda.com) have entered a second extended collaboration agreement for developing a renewable-chemical bioprocessing technology. The second phase of the project aims to accelerate commercialization of the target chemical. Arzeda reached a major deliverable in the previous engagement, which set the stage for BP to move to this extended agreement.

Archroma finalizes acquisition of BASF's stilbene-based OBA business

December 6, 2019 — Archroma (Basel, Switzerland; www.archroma.com) has completed the acquisition of BASF's stilbene-based OBA

(optical brightening agents) business for paper and powder detergent applications. The transaction includes BASF's manufacturing unit at Ankleshwar, India.

Huntsman to acquire foam manufacturer Icynene-Lapolla

December 6, 2019 — Huntsman Corp. (The Woodlands, Tex.; www.huntsman.com) plans to acquire Icynene-Lapolla, a North American manufacturer and distributor of spray polyurethane foam (SPF) insulation systems. Under terms of the transaction, which is expected to close in the first half of 2020, Huntsman will spend $350 million for the acquired business.

Indorama acquires California-based plastics recycling business

December 4, 2019 — Indorama Ventures Ltd. (IVL; Bangkok, Thailand; www.indoramaventures.com) signed a definitive agreement to acquire a 100% stake in Green Fiber International Inc. (GFI), a company that operates a plastics-recycling facility in Fontana, Calif. This facility produces primarily recycled polyethylene terephthalate (rPET) flake with a total capacity of 40,000 m.t./yr.

Umicore completes acquisition of Freeport cobalt-processing assets in Finland

December 2, 2019 — Umicore N.V. (Brussels, Belgium; www.umicore.com) has completed the acquisition of Freeport Cobalt's cobalt refining and cathode precursor activities in Kokkola, Finland, for a purchase price of $203 million. All regulatory clearances in relation to the transaction have been obtained.

Lanxess acquires Brazilian biocide manufacturer

December 2, 2019 — Lanxess AG (Cologne, Germany; www.lanxess.com) has acquired biocide manufacturer Itibanyl Produtos Especiais Ltda. (IPEL; Jarinu, São Paulo, Brazil). IPEL generates the majority of its sales with biocides and specialty chemicals for the paint and coatings industry.

Haldor Topsoe and Sasol enter collaboration agreement for gas-to-liquids technologies

December 2, 2019 — Haldor Topsoe A/S (Lyngby, Denmark; www.topsoe.com) and Sasol Ltd. (Johannesburg, South Africa; www.sasol.co.za) have entered into a collaboration agreement to jointly license their gas-to-liquids (GTL) technologies. As single-point licensors, Sasol and Topsoe will offer customers all necessary technology licenses and provide basic engineering, catalysts and hardware.

Mitsubishi Chemical to acquire ASB' s TPU business

November 26, 2019 — Mitsubishi Chemical Corp. (MCC; Tokyo; www.m-chemical.co.jp) will acquire the TPU business of AdvanSource Biomaterials Corp. (ASB; Wilmington, Mass.) though its U.S. subsidiary Mitsubishi Chemical Performance Polymers, Inc., which is headquartered in South Carolina. ASB's TPU products are used mainly for medical devices. ■

Mary Page Bailey

Particle Size Matters

With the right technology, chemical processors can obtain precise particle size and consistent material while improving throughput and quality

Particle sizing is an essential task in the chemical process industries (CPI) where achieving high-quality product efficiently and at a low cost is the name of the game. For this reason, appropriate size-reduction equipment is critical to overcoming process challenges that impede throughput, as well as acing new applications that require smaller, purer particles. Measurement and monitoring of particle size is also necessary to ensure that particles remain properly sized and distributed, as process changes can wreak havoc on particle size. For this reason, size reduction and analysis equipment providers are introducing solutions that help chemical processors achieve target particle sizes in a consistent manner with higher yields.

Many CPI companies receive, process and produce materials as powders and granules. Often, the particle size of these materials plays a crucial role in how well they may be stored, handled and processed and can greatly impact productivity, as well as quality of the product, says Brian Pittenger, vice president, Jenike & Johanson (Tyngsboro, Mass.; www.jenike.com). "However, it is not yet common for processors to have a well understood and controlled nature of the particle size distribution," he continues. "When I visit chemical producers, it is rare that they have mass balances through their process on a particle-size-distribution basis. In fact, it is very common for this aspect of their process to be out of control, as it is rarely monitored or measured."

And, this can be a problem, because many chemical conversion steps require control of surface-area-to-volume ratios of materials being processed or the reaction may not proceed as expected. "For nearly every unit operation — milling, blending, drying, centrifuging, compacting, agglomeration, as well as storage, feeding and conveying steps — a well-controlled particle-size distribution will nearly always result in more consistent product, higher throughput and less loss and waste, as well as fewer process upsets and unplanned shutdowns," explains Pittenger.

Pittenger reports that his firm is routinely asked to troubleshoot the process and find, as a root cause, the uncontrolled variations of the particle size distribution. "It may come from unplanned attrition or agglomeration of materials as they move through the process or, more frequently, as a result of particle segregation since little attention was given during design or operation to particle flow," he says. "Furthermore, once a process is in place, it is commonplace for it to be pushed well past its original design basis for either greater throughput or as a result of changing product expectations in the market. These increases are often made with little regard to the impact on particle size distribution. Processes are run faster, hotter and with shorter residence times and these changes almost always result in substantial unplanned changes to the particle size and distribution."

For this reason, properly considering the particle size and distribution throughout the lifecycle — from design through planned changes — greatly benefits a range of processes. However, this requires the ability to measure and understand particle-size distribution as part of the process just as well as any other critical process variable, says Pittenger.

Netzsch

FIGURE 1. To assist with pre-mixing, Netzsch introduced the Epsilon, a compact solution for producing homogeneous dispersions with reproducible quality in an inline process

Size reduction solutions

Because every process is unique, there is no "one size fits all" when it comes to size reduction. Many size-reduction equipment providers, as well as engineering firms like Jenike, offer experience and laboratory testing and trials to help select the correct equipment for the application and to troubleshoot size-reduction processes that have gone out of specification. Most are familiar with the challenges faced in the CPI, and while those vary as widely as the applications, there are a few common issues.

The need for higher throughput is one of the most frequently heard challenges. Often when a processor seeks higher throughput, they assume that it is necessary to go with

a larger or additional size reduction machine; however, advances in sieving and screening may allow them to achieve more throughput and yield without additional sieving processes, says Jeff Hochadel, president, HK Technologies (Salem, Ohio; www.clevelandvibrator.com). "Bigger is not always better when it comes to getting material through a screen," he says. "We can apply ultrasonic technology to the screen or other high-frequency sieving devices that can give them additional yield without going to a larger machine."

For example, the HK Ultrasonic Screen Deblinding System can convert existing gyratory screeners, sieves or sifters to an ultrasonic screener. The system is designed using an ultrasonic transducer attached to a frame or ring, preserving the integrity of the mesh screen and extending life in the field. The frame delivers a high-frequency, low-amplitude ultrasonic vibration that excites the screen and eliminates blinding of materials, such as ceramics, powdered metals, pharmaceuticals, powder coatings or additives on the screen deck.

However, just tweaking the machine itself is not always enough to improve throughput. Other glitches include issues with premixing, says Paul Trefny, laboratory manager and applications process advisor with Netzsch (Exton, Pa.; www.netzsch.com). "Proper premix is often a challenge," says Trefny. "A customer may be using high-shear dispersing and a blade diameter is incorrect or something else is happening that leads to ineffective premixing. When the material is not properly premixed, it can be difficult to reach the target size and can also lead to problems with the mill, such as pressure, temperature, pumping and processing issues. However, they can get 15 to 25% better efficiency out of their mill if the pre-mix is effective."

To assist with pre-mixing, Netzsch introduced the Epsilon (Figure 1), a compact solution for producing homogeneous dispersions with reproducible quality in an inline process. The dispersion process takes place in an atmospherically sealed processing chamber and is dust and emission free. The inline disperser is operated in circulation mode, whereby the powder can be fed from a bag via suction lance or bag feeding station. The machine operates similarly to a feed pump. Through optimal flow control, a negative pressure is created in the processing chamber during operation. This negative pressure is used to draw in the powder, where, in combination with appropriate powder delivery, introduction of external air is minimized.

Midwestern Industries

FIGURE 2. Midwestern developed the Electro-Lift to assist with the lifting of separator frames, eliminating the need for two people to remove each frame. Also, the Electro-Lift helps reduce downtime and can be used to inspect the screens to ensure quality control

Maintenance issues frequently impede throughput, as well, says Joe Bailey, sales manager with Midwestern Industries (Massillon, Ohio; www.midwesternind.com). "We get a lot of calls from customers who are having issues with the screen not performing as it should or that they aren't getting the throughput they used to," he says. "Sometimes the issue is blinding, which can be solved with anti-blinding technologies, but often it's a matter of changing the screen. Screens in a screener are wearable items, and they can be difficult and time consuming to change." To combat the problem, Midwestern developed the Electro-Lift (Figure 2) to assist with the lifting of separator frames, eliminating the need for two people to remove each frame. Also, the Electro-Lift helps reduce downtime and can be used to inspect the screens to ensure quality control. "The system can be used by one person who pushes a button and the screen lifts up, allowing them to easily slide it out and slide in another to save downtime and labor during screen changes."

Bühler

FIGURE 3. The MicroMedia Invicta is the latest version of Bühler's bead mill, which features a new process-chamber design and bead-separator system that delivers a 25% increase in efficiency and a 50% uplift in productivity in wet grinding applications

Tackling new applications

Many of today's applications, such as those in pharmaceuticals, life sciences, battery and electronics and solar cells, require smaller, purer particles. Fortunately, size reduction equipment is rising to the challenge. "Surface area reactivity is the main reason processors want to get to finer particle sizes, sometimes in the 1 to 3 micron range or smaller," explains Jeffrey Hoffman, vice president, with Paul O. Abbe (Wood Dale, Ill.; www.pauloabbe.com). "And in many of these applications, such as those for solar-cell materials, advanced ceramics and glass and cobalt used in porcelain coatings, they require very consistent particles with a narrow particle distribution range so that, at the end of the day, the processor has an end product that is consistent."

Other materials may require even smaller particles, says Frank Tabellion, director of global sales and marketing, grinding and dispersing technologies, with Bühler Group (Uzwil, Switzerland; www.buhlergroup.com). "There is also a need for particles between 100 and 200 nm in the fields of inks, raw materials for batteries and other industries," he says. "For instance, for ink jet printing, they require particle sizes between 100 and

Paul O. Abbe

Micromeritics

FIGURE 4. Paul O. Abbe makes its ball mills in a range of materials that are compatible with what is being processed. For instance, if the material is ceramic, the company makes the ball mill from compatible ceramic materials so that there is no chance of contamination

FIGURE 5. The Saturn DigiSizer II uses a state-of-the-art CCD detector containing over three million detector elements and unique design and data-reduction features to provide users with an extremely high level of resolution and sensitivity

200 nm to prevent clogging of the printing nozzles, and in lithium ion batteries, they require finer particles to improve battery performance. This trend toward finer and nanosize particles requires fine grinding and a lot of energy."

For fine-grinding applications, ball and bead mills are often the go-to technology. "The size reduction equipment needs to be able to handle very small beads in order to achieve nanodispersions," says Tabellion. "An additional benefit is that the smaller beads you are using, the more efficient the whole grinding process becomes, regarding energy efficiency."

Bühler recently introduced the MicroMedia Invicta (Figure 3), the latest version of its bead mill with a new process chamber design and bead separator system that is said to deliver a 25% increase in efficiency and a 50% uplift in productivity in wet grinding applications. The remodeled bead separation system and screen design reduce blockages and pressure buildup. This allows recirculation to be driven faster, speeding up overall flowrates by an average of 100%. In addition to helping achieve target particle size faster, this also improves process safety and reliability.

In many of these sensitive applications, says Abbe's Hoffman, contamination can be an issue. "In applications for solar cells and electronics, as well as many others, it is essential that there is no contamination coming from the mill," he says. "In any application where the end product has to be super conductive, insulating or pure, contamination is a huge concern. It's the equivalent to being in the medical industry and saying I have the correct drug for you, but the needle isn't sterile." For this reason, Abbe makes its ball mills in a range of materials that are compatible with what is being processed (Figure 4). "For instance, if the material is ceramic, we make the ball mill from compatible ceramic materials so that there is no chance of contamination."

Up-to-the-task instruments

When it comes to ensuring product quality, monitoring and measuring particle size and distribution is as important as getting the sizing right. "Processors need to know, with precision and accuracy, good information about particle size and distribution of sizes because not everything is going to be perfect," says Jeffrey Kenvin, technical director with Micromeritics (Norcross, Ga.; www.micromeritics.com). "Detecting when there's a problem, such as there being too many big particles, and trying to understand what is causing the problem when you're manufacturing something is essential because particle size issues can slow down the process, create problems with speed of the process, harm processing equipment and affect performance and quality of the final product. When there's a mistake or a problem, there is often a severe economic penalty for the processor."

Because processors must make consistent product, they need assurance that their particle sizes are within specifications, so their test methods have to be robust, dependable and representative of the product, explains Kenvin. "Digital control has dramatically improved the quality of laboratory instruments as it allows not only the measurement to be more accurate and repeatable, but also the device itself," he says. "If I buy one device to use in California and another for New York, they should both provide the same answer. Thanks to digital controls, the performance of the instruments has really leveled out and devices are very accurate and repeatable because they employ the same control algorithms and control devices."

However, accurate and repeatable results aren't the only thing processors are looking for. "Speed of analysis is also important for many processors, especially when they are monitoring and measuring particle size in order to make decisions about operating the process or quality control," says Maik Paluga, sales consultant, particle sizing, with Fritsch GmbH (Idar-Oberstein, Germany; www.fritsch.de). Fritsch introduced the Dynamic Image Sizer, which can be fed with dry powders or granules (between 20 µm and 2 cm) that are transported by a vibrating feeder and fall into the measuring zone. There, they pass between a camera and a flashing light source. Images are taken with a rate of up to 72 frames per second and transferred to the software that determines the outer perimeter of each particle. This

Horiba Instruments

FIGURE 6. The ViewSizer 3000 incorporates three variable light sources, allowing the instrument to select the optimum conditions for any sample analysis, overcoming limitations of conventional nanoparticle-tracking analysis when analyzing polydisperse samples and enabling a much larger range of particle sizes to be visualized

provides information not only about particle size, but also about particle shape. "The results they need can be achieved within minutes using this equipment versus spending hours waiting for the results of one traditional analysis."

And, the trend toward smaller particles requires instruments that provide a better understanding of smaller sizes, says Kenvin. "We are moving into a range where the smaller the particles get, the more challenging it is to rapidly determine size, which is critical when the technology is used in the process industries and they need results in a timely manner," he says. "So the challenge becomes the ability to provide a better understanding of smaller particle sizes, more precisely and in a timelier fashion."

He says dynamic light-scattering technology is a good solution for this type of monitoring. "For some time, progress in laser light-scattering technology led to faster analyses, but the quality of the measurement was limited. Recognizing the need for better detection capability, Micromeritics developed the Saturn DigiSizer, an instrument that employed a laser diode and modern charge-coupled device (CCD) detector to improve the sensitivity, resolution, reproducibility and repeatability of the laser light scattering particle sizing technique," he says.

Improving further, Micromeritics introduced the Saturn DigiSizer II (Figure 5). Using state-of-the-art CCD detector containing over three million detector elements and unique design and data reduction features, the latest version provides users with an extremely high level of resolution and sensitivity. The level of detail, accuracy and resolution enables the extraction of all available information from the static light scattering pattern. Users can now measure the same material on multiple instruments located at different locations around the world and obtain the same, highly detailed size distribution measurement on each instrument.

And, for applications with more advanced formulations that included mixed particle sizes, all of which are submicron, Horiba Instruments Inc. (Irvine, Calif.; www.horiba.com) introduced an instrument for nanoparticle tracking analysis, says Jeffrey Bodycomb, product line manager, particles characterization, with Horiba. "The latest technology in particle sizing is the advent of multi-laser nanoparticle-tracking analysis. This is a big improvement over the older, single laser systems that did not work well with the size distributions commonly encountered in proteins, nanoparticle synthesis, vaccines or viruses. Nanoparticle tracking lets users determine detailed size distribution of submicron particles with much better accuracy than traditional dynamic-light-scattering instruments. With appropriate choice of scattering volume, it is also a suitable tool for determining submicron particle concentration."

The company's ViewSizer 3000 (Figure 6) incorporates three variable light sources (blue, green and red), allowing the instrument to select the optimum conditions for any sample analysis, overcoming limitations of conventional nanoparticle tracking analysis when analyzing polydisperse samples and enabling a much larger range of particle sizes to be visualized. Furthermore, by introducing the sample in an easy-to-use (and clean) cuvetter, the ViewSizer 3000 is able to repeatedly "analyze and stir," giving more reproducible results. And, since the sample is viewed in a vertical orientation, it is suitable for visualizing processes such as protein aggregation or crystal dissolution. ■

Joy LePree

Focus on Motors and Drives

Siemens

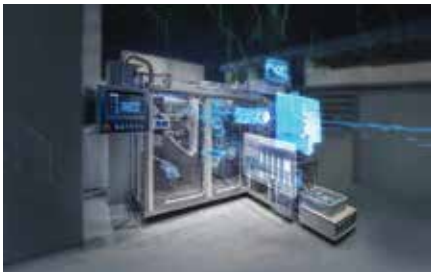

New version of drive-analyzer app now available

At SPS 2019 (Nuremberg, Germany; November 26–28), this company presented its latest solutions for smart and networked drive technology (photo). By networking entire drive systems, machine and plant builders, as well as users, can simulate machines and plant more accurately using digital twins, perform commissioning, reduce downtimes and therefore increase productivity. The new version V1.0 of the Analyze MyDrives MindSphere application (app) offers users new powerful diagram libraries for faster visualization. The new "Pan & Scan" function enables users to specify a precise timeframe for monitoring. Users can freely configure trend analytics. A new dashboard provides the key status information for all relevant drive components at a glance. — *Siemens AG, Munich, Germany*
www.siemens.com/digital-drives

Brother Gearmotors

IPM gearmotors that are small and run cool

IPMax (photo) is a line of lightweight, compact interior permanent magnet (IPM) gearmotors that are highly efficient with a wide synchronous speed range. IPM motors are suited for conveyors, fans and pumps, and are frequently used for factory automation, material handling, packaging and food processing. The gearmotors can operate fanless up to 1 hp, and do not require encoders for sensor control. When stopped, a servo lock feature holds the motor in position. IPMax gearmotors are 23% smaller than comparable IE3 motors, and run 24% cooler for longer lifespan, says the manufacturer. — *Brother Gearmotors, Bridgewater, N.J.*
www.brothergearmotors.com

Minarik Drives

Save costs, simplify sizing with this new servo system

The new Allen-Bradley Kinetix 5100 servo drive has multiple control modes available to support a wider range of high-speed, low-power motion-control applications. The drive can be used with a Micro800 controller, a Logix controller or even by itself, allowing original equipment manufacturers (OEMs) to choose how the product best functions in their applications. Bundling the drive, motor and cable together creates more competitive system pricing. With built-in safe torque off (STO), users can remove motor torque without removing power from an entire machine, allowing a machine to restart faster after it has reached a safe state. Dual-port EtherNet/IP also supports device-level ring topologies. — *Rockwell Automation, Inc. Milwaukee, Wis.*
www.rockwellautomation.com

Versatile new controls for brushless d.c. motors

The MDBL Series (photo) is a new family of configurable controls for brushless d.c. motors. MDBL drives control motors ranging from 90 to 280 V d.c., up to 5 A/1.5 hp, using either 115- or 230-V a.c. line sources. An onboard microprocessor allows for custom programming the MDBL Series for tasks as simple as changing the purpose of a jumper or trim pot, or as complex as programming an entire application-specific routine. The MDBL also seamlessly integrates PLC-like functionality into operations, eliminating the need for a separate PLC altogether or enhancing systems without PLCs. — *Minarik Drives, South Beloit, Ill.*
www.minarikdrives.com

New drives bring enhanced control to d.c. installations

Built on this company's all-compatible drive platform, the DCS880 (photo, p. 17) controls a variety of d.c. motor applications with unmatched safety, simplicity and interconnectivity. The new series of d.c. variable-speed drives (VSDs) allow users with a large installed base to get better performance from their existing systems. With the new DCS880 VSDs, users who are heavily invested in a d.c. system have the option to continue using d.c. technology while better aligning with modern a.c. advancements. The

Note: For more information, circle the 3-digit number on p. 50, or use the website designation.

d.c. VSDs are also easily integrated with the company's Ability monitoring services — a unified, cross-industry, digital offering that provides realtime data about drive status and performance from any location. Monitoring parameters include drive availability, environmental conditions and fault events. Optimized for safety, simplicity, and user-friendliness, the drives feature built-in functions, such as STO, which prevents unexpected startup of machinery. — *ABB, New Berlin, Wis.*
www.abb.com

The world's first 100-hp single-phase electric motor

The Belle single-phase motor (photo) uses Written-Pole technology to deliver a 100-hp single-phase motor that is compatible with readily available single-phase utility services. The utility-friendly starting and operating characteristics provided through the use of Written-Pole technology minimize voltage sags and flicker on long single-phase distribution lines. Ideal for industrial applications in areas where three-phase power is not readily available or cost-effective, this technology eliminates the need for phase converters or complex variable-frequency-drive (VFD) installations. Rated as a 100-hp, 460-V, 1,800-rpm electric motor, this design delivers 95.5% efficiency at rated load with a near-unity power factor. — *Single Phase Power Solutions, LLC, Cincinnati, Ohio*
www.sppowersoluitons.com

These slim hybrid motor starters extends motor life

The Crydom DRMS Series hybrid motor starters (photo) integrate the benefits of both solid-state and electromechanical-relay technologies to produce a compact device that can control electrical power delivery to motors as large as 4 kW. Suitable applications range from access control, packaging equipment, lifts and escalators to industrial process control and machine tooling systems. Unlike many motor starters of similar size, the DRMS Series offers features such as soft start, soft stop and an internal-mains disconnect relay in case of a fault. The starter's soft start/soft stop function allows for the gradual increase or decrease of power control, thereby extending motor life. Built-in overload protection eliminates the extra cost and space otherwise needed for an additional overload relay. The compact 22-mm wide DIN rail-mount motor starter package features an output rating of 9 A at 480 V a.c., 24 V d.c. control voltage and four easy-to-see LED status indicators. — *Sensata Technologies, Inc., Attleboro, Mass*.
www.sensata.com

This vertical inverter-duty motor is available off-the-shelf

To respond to the growing demand for variable speed motors used to drive vertical pumps in municipal and industrial applications, this company now stocks a line of totally enclosed-fan-cooled Corro-Duty Vertical HollowShaft Inverter Duty Motors (photo). These "U.S. Motors" brand motors are cast iron, and designed with full Class H insulating materials to withstand the steep-wave-front voltage impressed by the VFD waveform. They are designed to run smoother and cooler on inverter power supplies, which can lead to improved system efficiency and reliability. The motors are NEMA Premium Efficient, and are available in 5–300 hp, with two and four poles (3,600 and 1,800 rpm), and with frame sizes 184–449. — *Nidec Motor Corp., St. Louis, Mo.*
www.nidec-motor.com

Modular hybrid motor starters streamline installation

Contactron pro is a hybrid motor starter that simplifies wiring and safety integration. The auxiliary contact modules allow feedback of the motor state and implementation of self-sealing motor circuits. When used with the PSR-MC38 safety relay, the Contactron pro can easily permit a SIL 3/PLe group of emergency shutdowns via one interface. Like the original Contactron, the pro modules incorporate this company's Hybrid Technology, which offers three-phase motor switching up to 5 hp. Compared with traditional contactors, it reduces wiring time and space by up to 75%, says the company, adding that the device has a service life of up to 30 million switching cycles, which is up to ten times the service life of electromechanical solutions. — *Phoenix Contact USA, Middletown, Pa.*
www.phoenixcontact.com ■

Gerald Ondrey

ABB

Single Phase Power Solutions

Sensata Technologies

Nidec Motor

New Products

Hermetic-Pumpen

Expanded modular line of canned-motor pumps

This company has expanded its range of modular V-Line canned-motor pumps (photo) for the chemical and petrochemical industries. In addition to new accessories and more individualized documentation, the V-Line's performance range now also includes compatibility with aggressive media and lower fluid temperatures down to –50°C. In conjunction with modified bearing clearance, the V-Line is also suitable for pumping any type of potentially explosive refrigeration media. Previously, the units were available in stainless-steel or cast-steel design. Now, cast-steel housings can also be combined with stainless-steel impellers. The product range is suitable for application with pumping heads from 12 to 295 m; volumetric flowrates from 1.0 to 130 m³/h; fluid temperatures from –50 to 120°C; power ratings from 8 to 48 kW; and pressure ratings from 16 to 40 bars. — *Hermetic-Pumpen GmbH, Gundelfingen, Germany*
www.hermetic-pumpen.com

GE Digital

Edge-to-cloud data collection and accessibility

Proficy Historian 8.0 (photo) provides users with a scalable solution for data collection and aggregation across deployments of any size, extending data migration from edge to cloud. Updates to Version 8.0 include tag mapping, advanced trend analysis with annotations and the ability to define an asset model, allowing users to put data into context with business needs. Proficy Historian software is tightly integrated with this company's Proficy HMI/SCADA applications and Proficy Manufacturing Execution Systems. This integration enables operators to seamlessly manage machinery and plant processes. Also available is a Linux-based Proficy Historian that creates a standard time-series product for edge analytic applications. The Linux version of Proficy Historian pushes data to the plant level instead of polling from higher-level systems, providing a more efficient mechanism, according to the company. — *GE Digital, San Ramon, Calif.*
www.ge.com/digital

L.J. Star

LED illumination simplifies sight-glass setup

The capabilities of MetaClamp and MetaGlas sight-glass windows have been expanded with the addition of light-emitting diode (LED) lighting technology. Designed for sanitary or hygienic applications in the pharmaceutical, food, beverage, brewery and biotechnology industries, the new MetaClamp LED Ring Light Series SGL (photo) provides both illumination and viewing through the same window. This combination sight and light glass incorporates the MetaClamp system with MetaGlas safety windows. They can be used to view the interior of either new or existing sanitary-processing equipment, such as bioreactors, mixers, brew kettles, filters, tanks, hoppers, silos, agitators, separators, pipelines and other usually closed containers in non-hazardous areas. Unlike other devices that use separate viewing and fiber-optic light assemblies, the MetaClamp LED Light Ring mounts directly onto sanitary ferrules for use in combined sight and light ports (single port). The design is both less expensive and more durable for industrial settings, since it uses fewer sub-assembly components. The unit is approved for ambient temperatures ranging from 0 to 50°C at the cable entry gland. — *L.J. Star Inc., Twinsburg, Ohio*
www.ljstar.com

Endress+Hauser

Glass-free pH sensors with improved CIP stability

The new generation of ISFET sensors (photo) is made of unbreakable polyether ether ketone (PEEK), which offers maximum product safety, accuracy and much improved clean-in-place (CIP) stability. ISFET pH sensors can be used in any application where glass PH sensors are not desirable due to challenging process conditions or risk of breakage. The use of glass sensors is avoided in applications in the food-and-beverage or life-sciences industries, since entire production batches could become contaminated in the event of glass breakage. The ISFET sensors made of PEEK are available with three different reference systems. The new ISFET sensors, Memosens CPS47D and CPS77D, are equipped

to meet the strict demands of hygienic applications. They are said to deliver stable and reproducible measured values, even after sterilization and autoclaving up to temperatures of 135°C, and come with hygiene approvals for the food and life-sciences industries, such as USP, EHEDG and 3A. — *Endress+Hauser AG, Reinach, Switzerland*
www.endress.com

Stainless-steel tank covers for hygienic processes

LKD and LKDC tank covers securely fit the openings of high-, low- or non-pressure tanks, both above and below the liquid level. Two different models are offered for hygienic processes. The circular LKDC stainless-steel tank cover (photo) is used on top of tanks or containers. It is supplied with a replaceable, self-sealing double-lip seal to prevent fluids from spraying out, for example, during clean-in-place (CIP) and similar processes. The oval-shaped LKD stainless-steel tank cover is used on tanks or containers in various hygienic industries. For personnel entry, the cover can either be removed at the double hinge or swung out of the tank. The seal is not affected by positive or negative pressure in the tank. The LKD and LKDC inspection and personnel-entry ports are approved in compliance with the American 3-A Sanitary Standard and the U.S. Food and Drug Administration. The tank covers are available in 304 or 316L stainless steel with several options for seal materials and surface finishes. — *Alfa Laval, Lund, Sweden*
www.alfalaval.com

Customizable, automatic ingredient-batching systems

This company's Micro and Tote Batching Systems (photo) are customized, automatic ingredient-batching systems for both liquid and dry materials. These systems typically include supply bins, feeders, work platforms, automatic or manual bin refilling, liquid tank/pump skid equipment and the dry- and liquid-dosing automatic control system. Optional equipment may include raw-material bag lift equipment, dust collection and control for high-dust dry materials, batch-material conveying equipment (such as mechanical drag conveyor), lot tracking and traceability, barcode scanning and more. High accuracy can be attained — to within 0.001 lb or 0.5 g is possible, depending on applications. Liquid dosing includes high-accuracy Coriolis flow-metering devices and pumping systems. — *Sterling Systems & Controls, Inc., Sterling, Ill.*
www.sterlingcontrols.com

Feeding the USB port out of the control cabinet

With the new CU8210-M001 cabinet dome (photo), the USB port of an Industrial PC can be fed out of the control cabinet and still be well protected, establishing reliable and powerful wireless connections to the control computer without having to use attenuation-prone antenna cables. When combined with the appropriate CU8210-D00x USB 2.0 sticks, which are available for WLAN or 4G mobile communication, the cabinet domes support efficient and globally usable wireless solutions for PC-based control technology. The cabinet dome is designed to house industrial WLAN and mobile communication components and complies with IP 66 protection rating in the installed state. The components inside the housing dome, such as the USB 2.0 sticks for wireless communication, are completely protected against physical contact, dust, spray water and water jets. — *Beckhoff Automation GmbH & Co. KG, Verl, Germany*
www.beckhoff.de

Ultra-compact valves for bioprocessing applications

The new BioviZion valve (photo) is an ultra-compact model available in diameters ranging from 0.25 to 0.5 in. for sampling and low-flow bioprocessing applications. BioviZion valves include a mechanical thermal-compensation system wherein a sealing force is constantly applied to prevent external leaking over a range of temperature changes. A quick-change bonnet is said to significantly reduce maintenance time tenfold. A patented diaphragm stud enables simple and quick installation. The valves' high-strength stainless-steel studs avoid the challenges associated with small fasteners. — *ITT Engineered Valves, Seneca Falls, N.Y.*
www.engvalves.com

Alfa Laval

Sterling Systems & Controls

Beckhoff Automation

ITT Engineered Valves

Valley Forge & Bolt

Gardner Denver Petroleum & Industrial Pumps

Rite-Hite

SignalFire Wireless Telemetry

Built-in load monitor ensures correct loading to joints

Maxbolt load-indicating fasteners (photo) can reduce downtime, premature wear and catastrophic joint failures by continuously measuring and displaying the amount of tension in a bolt or stud. Each fastener has an accurate and durable load-monitoring device built in that indicates when proper load is achieved. During operation, technicians will know if load ever falls out of specification on any bolt, addressing the need immediately instead of waiting for critical equipment failure. Now, even inexperienced operators can assemble complex bolted joints with uniform clamp loads within ±5% of design specification. With Maxbolt devices, measurements are based on tension and the inaccuracies of torque control are eliminated, ensuring optimal initial conditions before an assembly is placed into service. — *Valley Forge & Bolt Mfg. Co. Phoenix, Ariz.*

www.vfbolts.com

A new pump for electric, gas and diesel-driven fleets

The new Thunder 5,000 hp Quintuplex pump (photo) is designed for duel-fuel gas engines, electric motors, diesel engines and gas-turbine direct drives. With stainless-steel construction and innovative geometry designed to minimize stress, the Thunder 5,000 hp Quintuplex pump features a range of next-generation fluid-end technologies. The pump's 11-in. stroke length meets or exceeds the pressure and flow output of high rod load/short stroke (8 in.) pumps, and can increase consumable life by 37%, says the company. The Thunder 5,000 hp Quintuplex pump is offered in combination with Redline Packing. This is the critical seal system in the heart of the pump, which substantially improves performance in harsh conditions, extends maintenance intervals, reduces downtime and ultimately increases profit margins for users, says the company. — *Gardner Denver Petroleum & Industrial Pumps, Houston*

www.gardnerdenverpumps.com

This new software streamlines logistics operations

Dok-Vu is a paperless software system for managing logistics operations (photo). The new software virtually eliminates the need for spreadsheets and two-way radios, connecting managers, materials handlers, yard personnel and carriers in real time. It allows users to get an at-a-glance status on every dock and trailer, while enabling carriers to avoid lines by checking themselves in and out and receiving text alerts on unload status. Managers using Dok-Vu can oversee appointments, monitor dwell times, and help keep docks fully utilized, gaining better control of charges, labor costs and shipping accuracy. Thanks to its intuitive loading-dock dashboard, Dok-Vu also allows managers to review current trends and historical data to make more data-driven decisions and help identify operational improvement opportunities. — *Rite-Hite Corp., Milwaukee, Wis.*

www.ritehite.com

Cellular sensor-to-cloud connectivity

The Ranger remote-monitoring system (photo) is a cellular transmitter that uses the LTE network to connect industrial sensors to the cloud for remote monitoring, control and alarming. By connecting directly to the cloud, the Ranger bypasses local networks to offer a more secure connection. The Ranger is designed to work with a wide range of sensor types and brands, making it easily integrated into industrial monitoring systems. Cloud connectivity removes barriers in collecting data from assets located in difficult-to-reach locations, such as pipelines in mountainous terrain or vast, remote tank farms. The Ranger comes equipped with this company's cloud interface, which allows users to remotely monitor assets, view trends and receive alarms either by text or email. It also provides for remote configuration and troubleshooting of the Ranger node and the sensor to which it is attached. — *SignalFire Wireless Telemetry, Hudson, Mass.*

www.signal-fire.com ■

Mary Page Bailey and Gerald Ondrey

Removal of Particulate Matter from Industrial Processes

Department Editor: Scott Jenkins

Controlling and reducing particulate matter pollution from industrial operations is a key environmental and human health objective. In chemical process industries (CPI) facilities, airborne particulate matter can result from combustion of fuels, or from process operations, such as dust from solids handling. Coal- and wood-fired boilers, and cement kilns are some examples of applications with high particulate levels upstream of the air-pollution control systems. This one-page reference outlines equipment and operational considerations for capturing particulate matter from industrial sources.

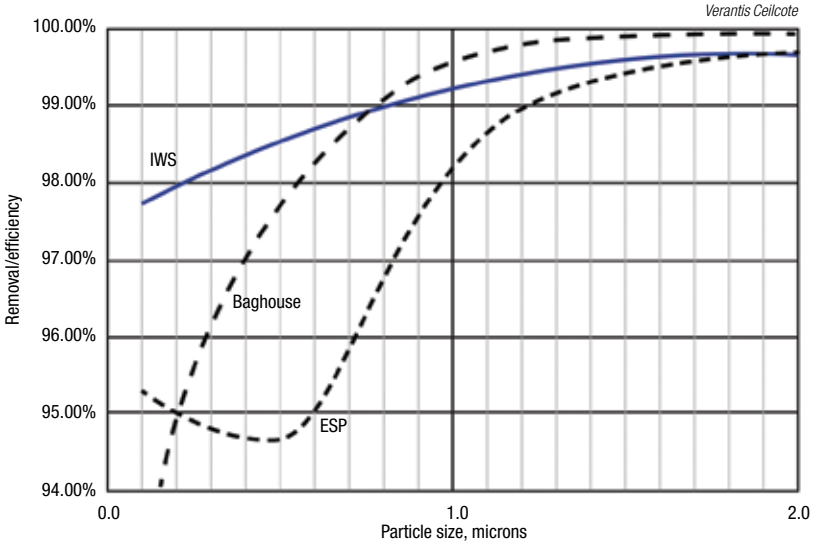

FIGURE 1. In this graph of particle size versus removal efficiency, three of the most commonly used air-pollution control devices experience a decline in collection efficiency as the particle size of the pollutants falls. This phenomenon is least pronounced for the ionizing wet scrubber (IWS)

Particle loading in fluegas

Particle loading in the fluegas from any industrial process is measured in grains/dry std. ft^3 (grains/dscf) or mg/dry std. m^3 (mg/dscm) or mg/normal m^3. The particle loading in the gas will vary widely depending upon a number of factors, including the gas velocity, particle size, particle density and the nature of the upstream process and feedstock. The smaller the particle, the more easily it is carried by the fluegas, even at relatively low gas velocity. As the gas velocity increases, larger particles can be carried by the fluegas stream, and the number of particles of all sizes that can be carried increases.

Removing particulate matter

Several operational approaches can remove solid particulate material from gases. Due to more stringent and complex regulations for multiple pollutants, different air-pollution control systems are frequently used in series.

Electrostatic precipitators (ESPs). ESPs use static electricity to remove soot (carbon from incomplete combustion) and ash from exhaust gas. Dirty gas is passed between two sets of electrodes in the form of metal plates, wires or bars. One electrode is charged with a negative voltage, which imparts a negative charge to solid particles being carried in the exhaust. A second set of electrodes is positively charged, and attracts the negatively charged pollutant particles, separating them from the exhaust gas stream. In a dry ESP, the removed particulate matter builds up on a collector surface, and is removed by mechanical vibration. In a wet ESP, the collecting electrodes are sprayed with water to remove the solid pollutants.

Wet scrubber. Wet scrubbers remove pollutants primarily through the impaction, diffusion, interception or absorption of the pollutant (either particulate matter or acid gases) onto droplets of liquid. The liquid containing the pollutant is then collected for disposal. An ionizing wet scrubber (IWS) combines the concepts of the ESP and the wet scrubber.

Venturi scrubbers. Venturi scrubbers are a type of wet scrubber that uses high-velocity streams of exhaust gas and water to atomize the liquid into fine droplets, which capture small particulate matter. Intensive mixing of the gas and liquid occurs in the throat of the venturi tube. The solid pollutant material is collected along with the liquid, while the cleaned gas escapes. With regard to particulate emissions, venturis tend to have limited ability to remove fine particles, and they experience exponentially higher pressure drops when forced to remove particulate matter. In recent years, with tighter U.S. Environmental Protection Agency (EPA) limits, the use of venturis as a standalone particulate-removal device has fallen out of favor.

Cyclones. Cyclone separators operate by creating a spiraling vortex of dirty gas inside a chamber. Solid particles carried by the gas are forced outward by centrifugal force as they travel around the chamber in a spiral pattern. Particles contact the walls of the cyclone and are collected at the bottom of the chamber, while cleaned gas leaves out of the top of the cyclone chamber.

Fabric filter baghouses. Woven cloth material captures particulate matter as gas flows through.

Removal efficiency

Each pollution-control device has its own characteristic operating curve. Figure 1 provides a comparison for an ionizing wet scrubber, filter baghouse and dry ESP. Note that the collection efficiency for all of these devices begins to fall off for smaller particles, with the ionizing wet scrubber having the least-rapid decay of its efficiency curve. Ionizing wet scrubbers are frequently used in series with two or three in a row, in part, to maintain removal efficiency during their required periodic wash cycle (a downstream unit operates while the upstream unit is being washed down). ■

Reference

Editor's note: Portions of this column are taken from: McGowan, T., Air-Pollution Control: Assessing the Options, *Chem. Eng.*, August 2016, pp. 62–70.

Production of ammonium nitrate

By Intratec Solutions

Ammonium nitrate (NH_4NO_3) is one of the most commercially important ammonium compounds, both in terms of production volume and usage. Its importance comes from the fact that the salt incorporates nitrogen, and makes it readily available in both forms used by plants and crops: nitrate ion and ammonia. While fertilizers are the main use of ammonium nitrate, it is also used in other industries, such as mining, military and civil engineering.

NH_4NO_3 is mainly commercialized in the following forms: aqueous solution, prills (pellets) and granules. The main grades are related to the content of nitrogen, usually ranging from 20 to 34.5 wt.% in solid forms.

The process

The process examined here (Figure 1) is a typical vacuum-neutralization process, which consists of two major sections: neutralization and finishing.

Neutralization. Initially, liquid ammonia is evaporated, superheated and sent to a neutralization reactor, along with a nitric acid solution and circulating ammonium nitrate solution. The ammonia reacts with nitric acid to produce ammonium nitrate. The reaction occurs under a slightly pressurized atmosphere, in order to prevent the ammonium nitrate solution from boiling and to minimize ammonia losses.

The ammonium nitrate solution, heated by the highly exothermic neutralization reaction, overflows to a flash vessel under vacuum, in which water is partially evaporated. The vapor obtained is used to heat neutralization feed streams, while the concentrated ammonium nitrate is split: a portion is circulated to the neutralizer, while the rest is fed to a second neutralizer with additional ammonia. The product from the second neutralizer is routed to a thermosyphon evaporation system, in which the solution is steam heated under vacuum. The ammonium nitrate melt obtained is directed to a prilling step downstream.

Finishing. The ammonium nitrate melt is initially mixed with a solution of dry magnesium oxide (MgO) to improve its storage properties. Subsequently, the ammonium nitrate melt is mixed with a prilling additive and sprayed at the top of a prilling tower. The ammonium nitrate prills are dried in rotating drums, then screened, cooled and coated with an anticaking agent. Off-specification material is recycled to the process. Finally, the ammonium nitrate prills are packed in bags and stored. Also, waste air from the prilling and drying steps is scrubbed before being discharged to the atmosphere.

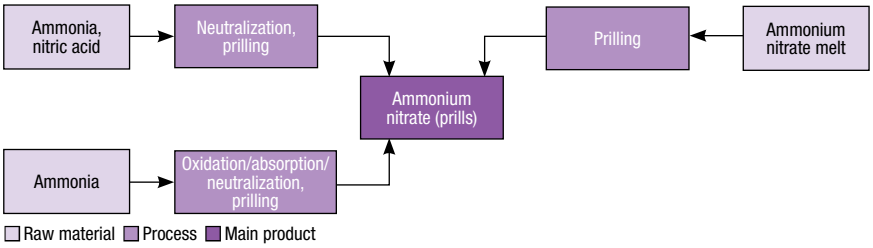

FIGURE 2. Ammonium nitrate can be produced via a number of different pathways

Production pathways

The commercial production of ammonium nitrate prills is mainly based on the neutralization reaction of ammonia and nitric acid. Ammonium nitrate production can be integrated with a nitric acid plant. In this case, ammonia is the only raw material. The diagram in Figure 2 presents the major production pathways for ammonium nitrate.

Economic performance

The total operating cost (raw materials, utilities, fixed costs and depreciation costs) estimated to produce ammonium nitrate was about $400 per ton of ammonium nitrate in the fourth quarter of 2015. The analysis was based on a plant constructed in the U.S. with the capacity to produce 400,000 metric tons per year of the compound.

This column is based on "Ammonium Nitrate Porous Prills Production Process – Cost Analysis," a report published by Intratec Solutions. It can be found at: www.intratec.us/analysis/ammonium-nitrate-production-cost. ■

Edited by Scott Jenkins

Editor's note: The content for this column is supplied by Intratec Solutions LLC (Houston; www.intratec.us) and edited by *Chemical Engineering*. The analyses and models presented are prepared on the basis of publicly available and non-confidential information. The content represents the opinions of Intratec only. More information about the methodology for preparing analysis can be found, along with terms of use, at www.intratec.us/che.

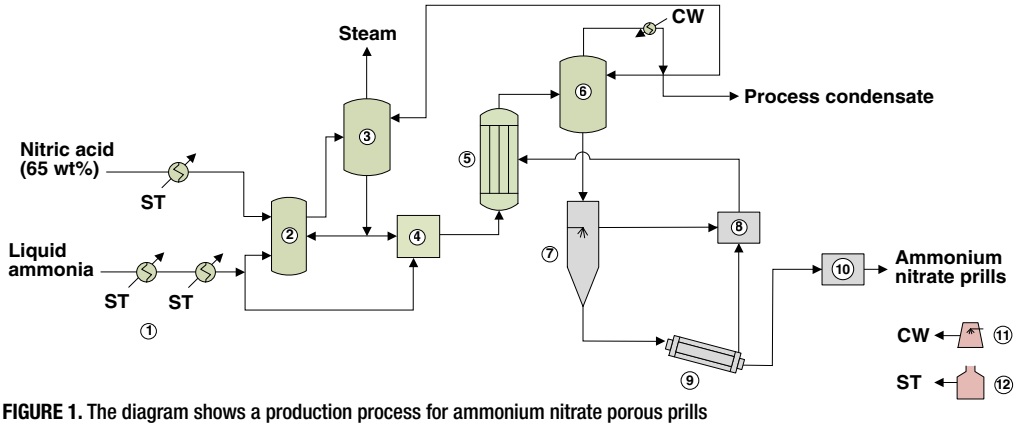

1. Vaporizer
2. 1st stage neutralizer
3. Neutralization flash
4. 2nd stage neutralizer
5. Evaporator
6. Evaporation flash
7. Prilling tower
8. Scrubbing system
9. Dryer
10. Finishing
11. Cooling tower
12. Boiler

CW Cooling water
ST Steam

FIGURE 1. The diagram shows a production process for ammonium nitrate porous prills

Gas Fermentation Leads Honored Achievements

The winning technology for the 2019 Kirkpatrick Chemical Engineering Achievement Award, along with the other finalist technologies, demonstrate how innovative engineering can tackle climate change and other challenges. All six technologies are described here

The six finalist technologies for the 2019 Kirkpatrick Chemical Engineering Achievement Award — including the winner, LanzaTech Inc.'s (Chicago, Ill.; www.lanzatech.com) gas-fermentation technology — represent the breadth of fields impacted by the chemical engineering profession. From industrial catalysis and petroleum refining to fermentation and bio-based plastics, the diverse set of technologies that garnered honor awards underlines the multidisciplinary nature of modern chemical engineering, and highlights the creativity and persistence of teams from across the globe.

The Kirkpatrick Award, given by *Chemical Engineering* magazine every other year since 1933, recognizes achievements in commercializing noteworthy chemical engineering technology. For a full list of previous award winners, see www.chemengonline.com/kirkpatrick-award/. The 2019 winning technology from LanzaTech, along with the five other finalist technologies — from Dow, Reliance, JohnsonMatthey, TechnipFMC and Braskem — are described here, along with some notes about recent progress.

Mary Page Bailey

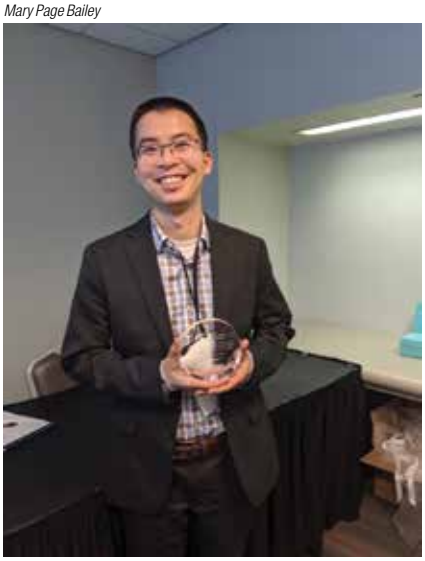

LanzaTech

FIGURE 1. LanzaTech's Allan Gao accepts the 2019 Kirkpatrick Award at the Chem Show in New York (left). A model of an ethanol molecule decorates the first commercial facility using LanzaTech's gas-fermentation process, a steel mill in China (right)

2019 AWARD WINNER

LanzaTech Gas fermentation

In traditional fermentation, microbes metabolize sugars to generate chemical compounds, such as alcohols. LanzaTech has developed a process featuring microbes that feed on carbon-rich gases, including exhaust gases, rather than sugar, and convert them into ethanol.

"The way we procure, use and dispose of carbon is fundamental to the wellbeing of our planet," says Allan Gao, senior process engineer at LanzaTech, "and we look forward to seeing more carbon recycling platforms deployed around the world."

Gao continues: "We're honored to receive the Kirkpatrick Award, and we appreciate the visibility of an award like this to highlight how technology and innovation can tackle climate change" (Figure 1).

The LanzaTech process offers an alternative to the Fischer-Tropsch (F-T) process, which has been used for decades to convert low-molecular-weight hydrocarbons that would otherwise be flared into liquid transportation fuels. F-T begins with synthesis gas from the gasification of hydrocarbons, coal or biomass. F-T has significant limitations, however, including the need for high pressures and the requirements that the synthesis be treated to remove diluents such as N_2 and CO_2, and remove contaminants that can poison the F-T catalysts. LanzaTech's process occurs at low pressures (less than 10 bars) and can operate on a wide range of H_2-to-CO ratios, converting the syngas to ethanol, which can then serve as a building block for other chemicals, such as rubber, plastics and fuels. Third-party assessments of the LanzaTech technology have shown greenhouse-gas-emissions reductions of over 70% compared to equivalent products from fossil carbon.

"Focus has been increasing on the use of non-food feedstocks to produce fuels, particularly in Europe and India,"explains Gao. "In addition to reducing greenhouse gas emissions, producing ethanol from industrial off-gas and waste positively impacts the environment in other ways. Also, the feedstock does not require land or additional resources to produce."

JohnsonMatthey

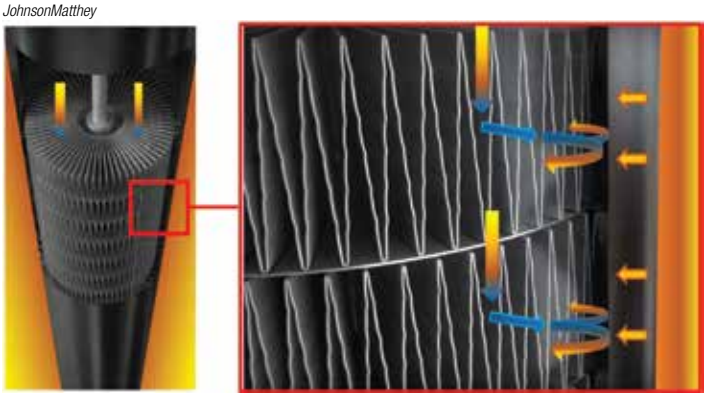

FIGURE 2. A novel catalyst for the steam-reforming of methane developed by JohnsonMatthey uses strips of alloy material folded and coated with catalyst material to improve heat transfer and reduce pressure drop

Dow

FIGURE 3. To allow for fast cure times in plastic laminate adhesives, the Dow Symbiex technology keeps the adhesives apart begins the cure phase only when the components of the laminate are joined

Microbes capable of utilizing CO, known as *acetogens* were first discovered in 1903, but had not been exploited in a commercial process prior to LanzaTech's work. The company was able to optimize the bacterium *Clostridium autoethanogenum* to produce ethanol at high selectivities from a wide range of gas feedstocks. LanzaTech's Gao says ethanol selectivities as high as 95% can be achieved stably while operating with feed gas of fluctuating composition. "The ability of the process to tolerate variable gas feeds is critical for utilizing these off-gas and syngas feedstocks," he says, which can come from steel-making and gasification of municipal solid waste and biomass.

Aside from the microbe, another development in the process was LanzaTech's bioreactor, which solves two unique challenges of gas fermentation. First, the bioreactor design enables high gas-to-liquid mass transfer of CO and H_2 at low pressure, "a critical requirement to enabling a cost-efficient high rate of reaction despite the low solubility of CO and H_2 in aqueous solutions," LanzaTech says. And second, the bioreactor is designed for concurrent consumption of CO and H_2.

LanzaTech and its industrial partners had been working to scale-up and commercialize the gas fermentation process since 2005, resulting in more than 100,000 hours of pilot- and demonstration-scale operating data at five sites co-located at industrial sites and operating on real industrial gases and syngas, Gao says. The pilot and demonstration experience led to the May 2018 startup of the first operating commercial gas-fermentation facility in the world: the Shougang LanzaTech commercial plant at the Jingtang Steel Mill in Caofeidian, Hebei Province, China.

The commercial plant in China has produced more than 10 million gallons of ethanol since startup in 2018. Ethanol from the plant is being used as a transportation fuel, but is also being converted into products, such as high-density polyethylene (HDPE) and ethylene glycol for use in the manufacture of polyethylene terephthalate (PET) plastic.

Plans are underway for the LanzaTech process to be deployed at other commercial sites, involving steel mill off-gas, refinery off-gas, and biomass and municipal solid waste syngas feedstocks. "The next two commercial plants in the pipeline are with Indian Oil Corp. and ArcelorMittal, operating on refinery off-gas and steel mill off-gas respectively, with the intent to construct further plants across their operations," says Gao.

LanzaTech is developing a number of downstream conversion routes for the use of the ethanol, including conversion to jet fuel, HDPE and a recently announced collaboration to convert ethanol into ethylene glycol for use in a high-tenacity yarn product, Gao says.

Converting alcohol to jet fuel

LanzaTech recently announced progress in scaling up its alcohol-to-jet (ATJ) platform. The company entered a partnership with the U.S Department of Energy's Pacific Northwest National Laboratory (PNNL; Richland, Wash.; www.pnnl.gov) in which PNNL developed a unique catalytic process to upgrade ethanol to alcohol-to-jet synthetic paraffinic kerosene (ATJ-SPK) and LanzaTech scaled up the process from laboratory to pilot scale.

After the April 2018 scaleup, ethanol was added as an approved feedstock in ASTM D7566 Annex A5 (Standard Specification for Aviation Turbine Fuel Containing Synthesized Hydrocarbons for ATJ-SPK), and in October 2018, it was used to power a commercial flight with Virgin Atlantic.

Now plans are underway to build a demonstration-scale facility for the jet fuel made ultimately from captured exhaust. Michael Berube, DOE deputy assistant secretary for transportation, announced that DOE is negotiating with LanzaTech for a $14 million investment in a demonstration-scale integrated biorefinery at LanzaTech's Freedom Pines site in Soperton, Ga.

The PNNL/LanzaTech ATJ process can use any source of sustainable ethanol for jet fuel production, including ethanol made from recycled pollution. The flexibility of the technology to utilize a variety of local waste feedstocks attracted the attention of Japan's All Nippon Airways (ANA), resulting in an offtake agreement with LanzaTech signed in 2019, allowing ANA to purchase sustainable aviation fuel from LanzaTech's process.

Following this agreement, ANA, Mitsui & Co. and JXTG Energy have been selected by the New Energy and Industrial Technology Development Organization (NEDO; a Japanese public research organization) to conduct a feasibility study on scaling the LanzaTech ATJ platform in

Japan. The partners aim to establish a sustainable domestic supply chain for ATJ, key to achieving full commercial deployment in Japan.

ANA and Mitsui & Co. kicked off the project by conducting a Boeing 777-300ER ferry flight using sustainable aviation fuel made from recycled carbon on October 30, 2019. As the fuel producer, LanzaTech worked closely with all partners, advising how best to transport and blend the fuel for loading on the aircraft.

"Sustainable aviation fuel reduces carbon emissions by up to 80% and is a key element of the industry's climate action strategy," says Sheila Remes, vice president of strategy at Boeing Commercial Airplanes. "ANA's flight demonstrated that sustainable fuel blends with conventional fuel without the need for any changes to the airplane, engines or airport fueling infrastructure."

LanzaTech's carbon capture platform for sustainable aviation fuel is now poised for scale up in the U.S. and Japan. In the U.K., LanzaTech is a shortlisted applicant for a grant from the U.K. Department for Transport (DfT) through the Fuels for Flight and Freight Competition (F4C). This grant would support deployment of the technology in the U.K.

2019 HONOR AWARDS

JohnsonMatthey Catacel SSR

Most hydrogen for industrial use in petroleum refining, ammonia production and other applications is made via steam-reforming of natural gas over catalyst-impregnated ceramic pellets. Recent increased demand for hydrogen has pushed operators of steam methane reformers (SMRs) to maximize capacities, however, doing so can often lead to limitations in temperature, pressure and feed flows.

The current design of catalyst pellets improves catalyst activity and heat transfer, but further improvement is blocked as gains come with higher pressure drop. To boost catalyst performance, Johnson Matthey (JM; London, U.K.; www.matthey.com) has developed an innovative alternative to pellets: CATACEL SSR, a nickel-catalyst-coated metal foil technology that has been proven to increase catalyst activity and heat-transfer while simultaneously decreasing pressure drop by up to 20%. In fact, increases of 15–20% have been observed in plant throughput rates.

CATACEL SSR are designed to replace catalyst pellets in existing reformer tubes without the need for new capital investment. The structured foil units use alloy strips, engineered into a series of V-shaped bends (Figure 2), that the company calls fans, onto which the catalyst material is coated. The fans are stacked into mechanical assemblies that fit inside of the reformer tube. JM's proprietary catalyst coating technology allows the catalyst to durably attach to the fans' thin metal foil surface covering a high surface area. The stacked fans deliver superior heat transfer by intentionally jetting the gas on the internal surface of the reforming tube, rather than relying on the random flow of gas through a pellet bed. CATACEL SSR technology for steam-methane reformers enables gains in process performance that are not achievable with conventional pellet catalyst technologies, JM says.

Dow Symbiex

Flexible food packaging often uses different polymer materials layered together to form laminates that exhibit the full range of properties required for mechanical performance and food-contact regulations. Lamination adhesives are used to bind the layers together. According to Dow Packaging & Specialty Plastics (Dow; Midland, Mich.; www.dow.com), the trend has been toward faster-curing adhesives because they allow operational advantages (faster time to market and lower warehousing costs). Dow's Symbiex technology speeds the curing times for multilayer packaging.

Developed along with machinery manufacturer Nordmeccanica NA (Hauppauge, N.Y.; www.nordmeccanica.com), Dow's Symbiex overcomes a major challenge for plastic laminate adhesives, which is to balance the need for fast curing with the need to maintain easy processing.

The "pot life" of an adhesive refers to the time it takes for the mixed adhesive to increase its molecular weight to a point where it compromises the quality of the laminate in which it is used. For practical processing, it is desirable to have a long pot life, so operators can stop and start the machine between jobs without risking product quality. But once the adhesive is applied in the laminate, the imperative switches to fast curing time.

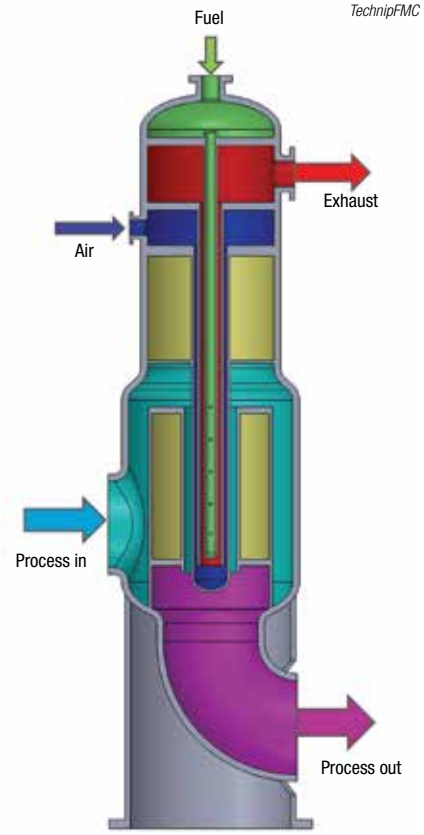

FIGURE 4. The Direct Heating Unit (DHU) uses flameless combustion, and is safer than a traditional fired burner system, with less emergency shutdowns, according to the developer TechnipFMC

The new lamination concept effectively separates the two components of the adhesive until they are actually together within the laminate. The cure only begins when the two coated films are brought together to form the multilayer film, and not before, so a convenient pot life is maintained, while a fast cure is achieved once the adhesive components join with in the plastic laminate, Dow says.

To make the system work, Dow and Nordmeccanica had to rethink and redesign the lamination machinery (Figure 3), while also developing modifications to the adhesive chemistry. The final system achieved improved pot life (4–6 h versus 20 min

Reliance

FIGURE 5. Benzene levels in FCC gasoline at the Reliance refinery in Mumbai have dropped to 0.05% and benzene recovery is 99%

for conventional adhesive technology), as well as accelerated curing time (less than one day versus 5–8 days with conventional technology.

TechnipFMC Direct-Heating Unit

The TechnipFMC (Houston; www.technipfmc.com) Direct Heating Unit (DHU) is a groundbreaking technology for adding heat to high-temperature processes. Unlike conventional furnace burners, where fuel and air are combined at a single point and a flame is present, fuel in the DHU is added incrementally to a high-velocity air stream via multiple injections over an extended reaction zone. As a result, the fuel reacts in a controlled manner at significantly lower temperatures than classic combustion and without a visible flame.

The concept of flameless distributed combustion was developed in the 1990s by Shell Oil for use in wellbore heaters for enhanced oil recovery. TechnipFMC licensed the technology from Shell for further development and application of the technology to process heating in styrene manufacturing.

The DHU consists of multiple sets of four concentric tubes, where a fuel-containing tube is the innermost and is surrounded by a reaction tube where the fuel and air combine. The fuel flows outward into the reaction zone through a precise pattern of orifices arranged along the length of the process-heating zone (Figure 4). Since the reaction air is preheated in the air tube, which Is the third concentric tube, by contact with the reaction tube, it enters the reaction tube at temperatures above the autoignition temperature of the fuel, which also has been pre-heated. Air and fuel are mixed and reacted continuously between the reaction tube and fuel tube, and the products flow up to the exhaust channel. The process fluid enters the DHU through a side nozzle and flows downward in the annular space between the outside of the air tube and the inside of the process sleeve, which is the fourth and outer most concentric tube. The process feed absorbs the heat released by the reacting fuel through both convection and radiation.

TechnipFMC says the DHU is far safer to operate than a traditional fired heater and has fewer emergency shutdown switches. In addition, the use of a DHU in styrene manufacturing reduces capital cost requirements, enables significant reductions in energy consumption in the process, and is operated more like a heat exchanger than a fired heater.

Along with Total Petrochemicals, TechnipFMC installed a DHU demonstration unit at Total's Cosmar Styrene Plant in Carville, La. After meeting the objectives for the DHU demonstration unit in over 10,000 hours of operation, a full-scale DHU was installed at an existing styrene production plant in Truinfo, Brazil. Videolar-INNOVA S.A. (INNOVA) recently started up the DHU at INNOVA's styrene plant, the first commercially operating example of the DHU technology in the world. INNOVA industrial director Sergio de Oliveira Machado states, "The DHU technology has surpassed our expectations and we are very pleased with how the project was completed with full cooperation from TechnipFMC's Badger Technology."

A second commercial-scale application of the DHU technology has also started up, TechnipFMC says.

The DHU technology was jointly developed with Total Petrochemicals and Shell Catalysts, and Technologies, and is licensed through TechnipFMC's Badger Process Technology Group. DHU technology is now routinely incorporated as part of the Total/Badger styrene technology for grassroots and revamp applications, TechnipFMC says.

Reliance benzene/gasoline

U.S. EPA regulations restrict the average benzene level in gasoline to 0.62%. To meet the requirement, Reliance Industries Ltd. (RIL; Ghansoli, India; www.ril.com) and CSIR Indian Institute of Petroleum (Dehradun, India; www.iip.res.in) jointly developed the world's first technology for processing the C6 heart cut of FCC (fluid catalytic cracking) gasoline. The technology is based on the principles of extractive distillation and does not need a pre-processing step to saturate di-olefins and reduce reactive impurities (chlorides, oxygenates, metals and others). The method not only produces EPA-compliant gasoline but also recovers high-purity benzene.

The technology features the most thermally and chemically stable and tunable solvent system for handling reactive impurities in FCC gasoline, along with an innovative and proprietary process configuration that minimizes solvent loss and utility requirements while maximizing product purity and yield.

The first commercial unit using this technology operates at RIL's petrochemical complex in Jamnagar, India (Figure 5). The benzene content of the raffinate (gasoline) has been consistently below 0.05%, while benzene recovery has exceeded 99% while producing extract with more than 98% benzene, RIL says. Patents for the technology have been granted in several countries.

Braskem renewable EVA

Braskem (Sao Paulo, Brazil; www.braskem.com.br) developed a process for renewable ethylene vinyl acetate (EVA) along with the footwear company Allbirds Inc. where sugarcane, instead of oil, was used as the raw material. Conventionally, EVA is produced from petroleum-derived ethylene. With input from a number of sources, Braskem developed a new resin to produce a range of EVA and EVA rubber products in a plant originally designed to produce ethylene. The first commercial product to use the new EVA is a line of flip-flops. ■

Scott Jenkins

Evaporators: Design Concepts and Equipment Selection

This primer provides guidance on key aspects to consider when designing and specifying evaporators, which are used in a diverse array of industrial sectors

Alan Gabelman
Gabelman Process Solutions

SPX SPX API Heat Transfer

FIGURE 1. Evaporators are used in a wide variety of process applications, and there are many styles of equipment in use today

Industrial evaporators are used to remove a solvent from a non-volatile solute to obtain a concentrated solution of the solute. This article focuses on evaporator heat-transfer fundamentals and other introductory concepts, as well as types of evaporators (Figure 1), including advantages, disadvantages and suitable applications of each.

In most applications, the heat source for evaporation is condensing steam. The concentrated product is aptly called concentrate, or thick liquor. The solvent that is removed is condensed to form process condensate, or simply condensate. With the exception of agitated thin-film units, the solvent is usually water, and this is assumed in most of the discussion that follows. The valuable discharge stream is almost always the concentrate, while the condensate is used for cleaning, recycled as process water, or simply discarded. The notable exception is the evaporation of seawater to obtain potable water, a process that is often part of a hybrid process with reverse osmosis. Evaporators are used in numerous industries, including food, chemicals, paper and textiles, and several significant applications are listed in Table 1.

EVAPORATOR DESIGN

The challenge faced by the evaporator designer is to provide the amount and configuration of heat-transfer surface such that, when presented with the feed material at the intended process conditions, leads to efficient removal of water (or other solvent) at a rate that meets the production demand. Traditionally, an evaporator heat-transfer surface is tubular, but flat plates are also commonly used. Both types of heat-transfer surface are packaged in a variety of evaporator types, such as film evaporators, forced circulation evaporators and others. Sometimes these evaporators contain energy-saving features, such as multiple effects or vapor recompres-

IN BRIEF

TABLE 1. SELECTED INDUSTRIAL APPLICATIONS FOR EVAPORATORS

Process/product	Description
Sugar	Used to concentrate crystallizer feed
Amino acids	Examples include lysine (used as animal feed) and glutamic acid (the acid form of monosodium glutamate, the popular flavor enhancer)
Fruit and vegetable juices	These include apple, orange, tomato, beet, grape, lime, mango, pear and pineapple juice
Milk	The product is commonly known as condensed or evaporated milk
Cheese whey	This is the liquid obtained upon separation of the curd
Various chemicals	Examples include titanium sulfate, ammonium nitrate, ammonium sulfate, barium salts, sodium hydroxide (caustic soda) and glycerin
Black liquor in pulp mills	In the production of pulp that is in turn used to make paper, black liquor is the slurry from the digester. The so-called weak black liquor is concentrated to aid in recovery of valuable chemicals
Effluent from textile dyeing	Evaporator condensate is reused, while the concentrate is fed to a downstream precipitation process to recover salts used for dyeing, which are in turn reused or sold

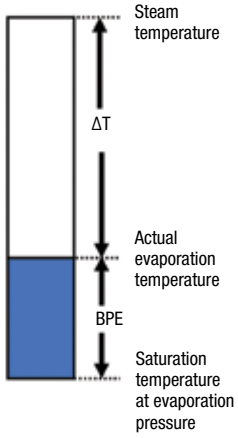

FIGURE 2. Boiling point elevation (BPE) erodes the temperature driving force, requiring more heat transfer area for a given evaporation load

sion. The preferred type of evaporator and, if appropriate, energy conservation technology, depends on numerous factors, including physical properties, required capacity, initial and final concentrations, foaming tendency, fouling tendency and heat sensitivity.

Important physical properties to consider for evaporator design are density, thermal conductivity, boiling point elevation (BPE), heat capacity, heat of vaporization and viscosity. To further complicate the design challenge, these physical properties can change significantly as the concentration increases. For instance, often the feed has a water-like viscosity, but the concentrate is a heavy syrup. The effect of temperature on physical properties must also be considered. Foaming can be a problem if organic compounds, such as protein (for example, in fermentation-derived products), are present. Chemical antifoams can help, along with extra headspace in vapor-liquid separators. Fouling may be caused by organic or inorganic species, with appropriate cleaning protocols available for each.

The evaporator design variable is heat-transfer area, which is specified to provide the required evaporation capacity, Q. Area (A) is calculated using the familiar capacity equation, shown in Equation (1), where U is the overall heat-transfer coefficient and ΔT is the temperature driving force:

$$A = Q/U\Delta T \qquad (1)$$

In evaporators, ΔT is not as straightforward as a simple difference between two fixed

NOMENCLATURE

A	Heat transfer area (ft^2)
C_P	Constant pressure heat capacity (Btu/lb-°F)
H	Enthalpy (Btu/lb)
m	Mass flowrate (lb/h)
Q	Heat duty (Btu/h)
T	Temperature (°F)
U	Overall heat transfer coefficient (Btu/h-ft^2-°F)
x	Mass fraction of solids

Subscripts

C	Steam condensate
F	Feed
P	Evaporator product (concentrate)
S	Steam
V	Vapor

Greek letters

λ	Latent heat of vaporization (Btu/lb)

temperatures, because temperature profiles are complex. BPE and pressure drop result in a change in temperature upon travel along an evaporator tube or plate. For purposes of design, ΔT is taken as the difference between the temperature of the condensing steam and the emerging concentrate, even though the actual ΔT varies along the length of the heat-transfer surface.

As illustrated in Figure 2, BPE erodes the temperature driving force, requiring more heat-transfer area for a given evaporation load. BPE can be estimated using Dühring's rule, which says that the boiling point of a given solution is a linear function of the boiling point of pure water at the same pressure. An example is the Dühring plot for aqueous sodium hydroxide shown in Figure 3, which contains concentration as a parameter. Note that for concentrated solutions, the BPE is considerable.

An evaporator must remove a specified amount of water from the feed per unit time, bringing the solids content to some target level. This requirement, along with the thermal condition of the feed and its physical properties (heat capacity and heat of vaporization), determine Q. The temperature driving force is set by the steam temperature and the boiling point of the process material at the chosen operating pressure. There are a number of considerations in choosing the operating pressure, which is usually below atmospheric. A lower pressure (higher vacuum) results in a lower temperature, which is important with heat-sensitive products, such as fruit juices. Moreover, the lower temperature offers a greater temperature driving force, allowing a given capacity to be achieved with less heat-transfer area. On the other hand, vacuum generation is a

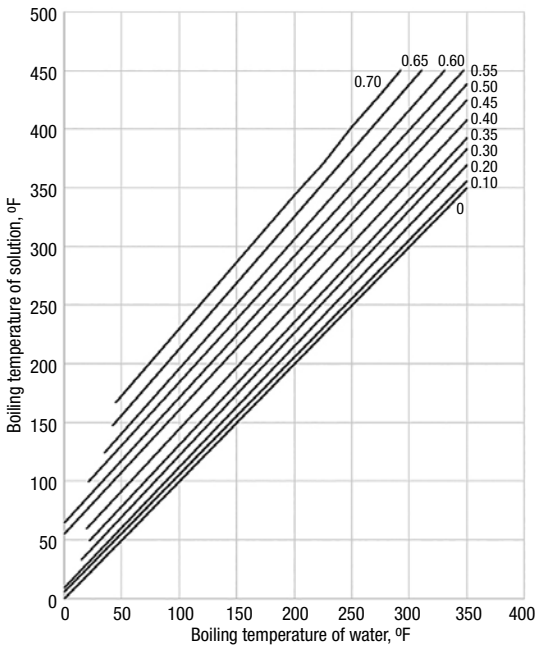

FIGURE 3. This Dühring plot for aqueous sodium hydroxide is used to determine the boiling point elevation. The parameter is mass fraction NaOH. Redrawn from data given in Ref. 3

cost, and the higher the vacuum, the higher the cost. Also, lower pressure means lower vapor density, and vapor piping needs to be larger to accommodate the corresponding increase in volume. For some viscous products, the minimum temperature is determined by the need to limit the viscosity and maintain a pumpable concentrate. Finally, the pressure must be high enough to allow a sufficient difference between the evaporation and cooling-water temperatures at the condenser.

Heat-transfer coefficients are well known for common applications, such as concentration of orange juice or aqueous sodium hydroxide. For less common situations, there are correlations that relate heat transfer coefficient to physical properties, tube or plate geometry and operating conditions [*1*, *2*]. As an alternative to published correlations, equipment manufacturers are more likely to use their own proprietary methods. Heat-transfer coefficients can also be determined experimentally [*2*]. Values range from 100 to 1,000 Btu/h-ft^2-°F (570–5,700 W/m^2-°C). In general, values are higher with lower viscosity and faster-moving fluids.

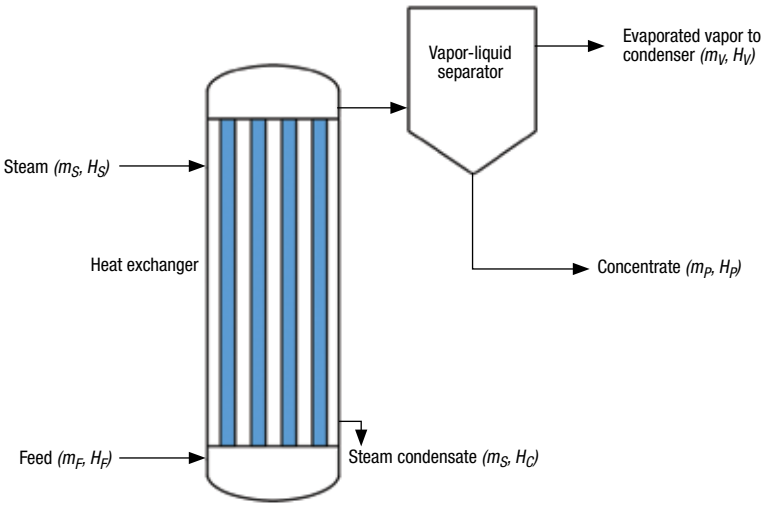

FIGURE 4. This simple schematic diagram provides a basis for development of evaporator mass and energy balances

Mass and energy balances

A simple schematic diagram of an evaporator is shown in Figure 4. The overall and component mass balances are given by Equations (2) and (3):

$$m_F = m_P + m_V \quad (2)$$

$$x_F m_F = x_P m_P \quad (3)$$

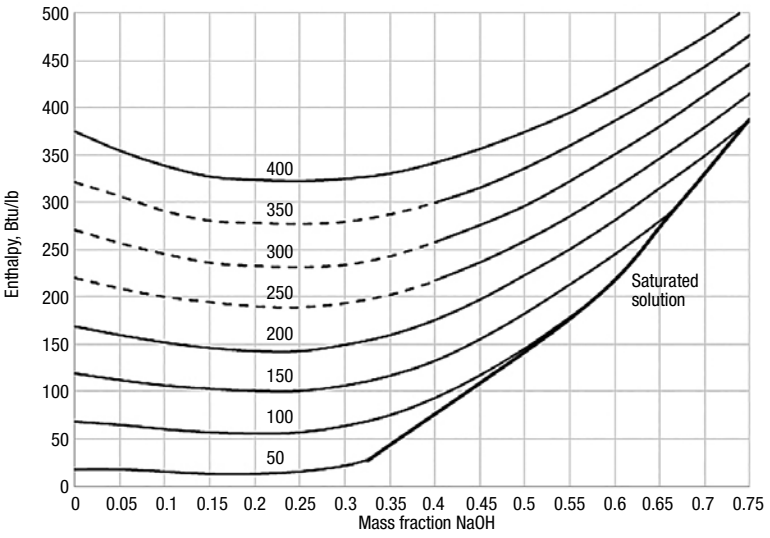

FIGURE 5. This enthalpy-concentration diagram for aqueous solutions of sodium hydroxide can be used for evaporator heat-balance calculations. The parameter is temperature in °F. The dashed lines are extrapolated values. Redrawn from data given in Ref. 3

Equations (2) and (3) are combined to obtain the useful expression for the evaporation rate shown in Equation (4):

$$m_V = m_F[1 - (x_F/x_P)] \quad (4)$$

The general form of the energy balance, assuming negligible heat loss, is given in Equation (5):

$$m_S H_S + m_F H_F = m_s H_c + m_V H_V + m_P H_P \quad (5)$$

Note that the mass flowrates of steam and steam condensate are the same. Steam condensate should not be confused with process condensate, which is the water (or other solvent) removed from the feed during the evaporation process. It is convenient to rearrange Equation (5) to obtain the expression for the heat duty shown in Equation (6):

$$Q = m_S(H_S - H_C) = m_V H_V - m_F H_F + m_P H_P \quad (6)$$

For a situation with saturated steam and no condensate sub-cooling, $H_S - H_C$ is the latent heat of vaporization, λ_S, which is approximately 1,000 Btu/lb for water. More accurate values may be obtained from the steam tables, available either in handbooks or online. Steam superheat and condensate sub-cooling are usually much smaller than latent heat and can be neglected for estimating purposes. If more accuracy is desired, enthalpy of superheated steam is also given in the steam tables, and sub-cooled condensate enthalpy can be calculated using the familiar sensible heat equation, shown in Equation (7):

$$H_C = C_{PC}(T_C - T_{ref}) \quad (7)$$

The reference temperature is taken as 32°F, the same as in the steam tables. The right-hand side of Equation (6) is the most general form of the heat balance, and it must be used for materials with significant heat of dilution. Examples include sodium hydroxide, sulfuric acid and calcium chloride. For some such systems, designers can use enthalpy-concentration diagrams, like the one shown in Figure 5 for sodium hydroxide. This diagram gives enthalpy as a function of the mass fraction of sodium hydroxide (NaOH), with temperature as a parameter. With no heat of dilution, the

FIGURE 6. This flowsheet shows just one of the numerous ways to operate a batch evaporation process. Controls are mostly manual, but like any chemical engineering unit operation, the degree of automation can be totally manual, highly automated or anywhere in between

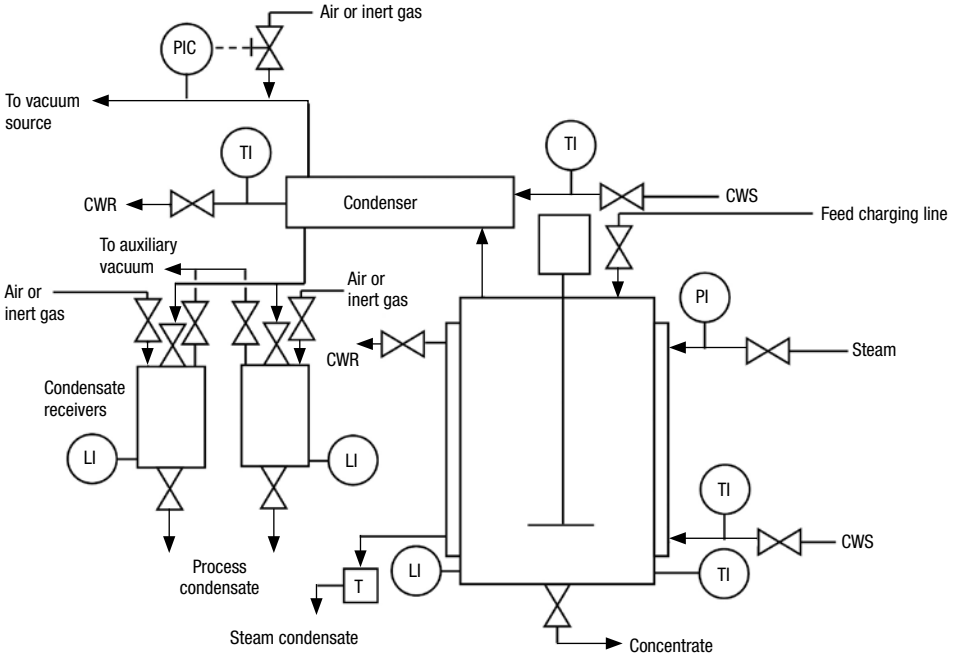

CALCULATION EXAMPLE

Consider an example where 20,000 lb/h of 12 wt.% sodium hydroxide at 70°F is concentrated to 50 wt.%, using an evaporator with a heat-transfer area of 2,500 ft^2. The heat source is saturated steam at 30 psig, and the pressure on the process side of the evaporator is 2 psia. We want to determine the heat load, the steam usage and the overall heat-transfer coefficient, assuming that we can neglect any heat loss or condensate sub-cooling.

Heat load

Because we expect the heat of solution to be significant, the heat duty is calculated using Equation (6), the more general form of the heat balance. From Equation (4), the evaporation rate is:

$m_V = 20{,}000\,(1 - (0.12/0.50)) = 15{,}200$ lb/h

The product flowrate is determined by the simple mass balance from Equation (2):

$m_P = 20{,}000 - 15{,}200 = 4{,}800$ lb/h

From the saturated steam tables, the saturation temperature at 2 psia is 126.0°F. The boiling temperature of 50% sodium hydroxide, found using Figure 3, is 200°F. From Figure 5, H_P, the enthalpy of 50% sodium hydroxide at 200°F, is 222.1 Btu/lb, and H_F, the enthalpy of 12% sodium hydroxide at 70°F, is 33.7 Btu/lb. H_V is obtained from the superheated steam tables, which give a value of 1,149.5 Btu/lb for steam at 2 psia and 200°F. Substituting into Equation (6) gives the following value for Q:

$Q = 15{,}200\,(1{,}149.5) - 20{,}000\,(33.7) + 4{,}800\,(222.1) = 1.786 \times 10^7$ Btu/h

Steam usage

The steam usage is also obtained from Equation (6), with $(H_S - H_C) = \lambda_S$ because both the incoming steam and the condensate are saturated (no superheat or subcooling). From the saturated steam tables, the latent heat of vaporization at 30 psig is 929.0 Btu/lb. From Equation (6), m_S is determined:

$m_S = Q/(H_S - H_C) = Q/\lambda_S = 1.786 \times 10^7/929.0 = 19{,}230$ lb/h

Overall heat-transfer coefficient

The overall heat-transfer coefficient (U) is calculated using Equation (1). The temperature of saturated steam at 30 psig, needed to determine ΔT, is 274.0°F from the saturated steam tables. Applying Equation (1) gives the following solution for U:

$U = Q/A\Delta T = 1.786 \times 10^7/(2{,}500\,(274.0 - 200)) = 97$ Btu/h-ft^2-°F ❑

isotherms would be straight lines rather than the curves seen in the diagram. Note that the isotherms terminate at the saturated solution curve, although they could be extended to handle precipitated solids if desired [3]. For systems with negligible heat of solution, Equation (6) becomes the expression shown in Equation (8):

$$Q = m_S(H_S - H_C) = m_F C_{PF}(T_{F,sat} - T_F) + m_V\lambda_V \quad (8)$$

The first term on the right-hand side is the sensible heat needed to raise the temperature of sub-cooled feed (the typical case) to the saturation, or boiling, temperature. For the latent heat of vaporization, λ_V, the value in the steam tables at the evaporation pressure is usually used, although the actual value is slightly different when BPE is significant [3].

EQUIPMENT SELECTION

As stated previously, the preferred type of evaporator depends on numerous factors, including physical properties, required capacity, initial and final concentrations, foaming tendency, fouling tendency and heat sensitivity. The following sections detail various types of evaporators and provide guidance for best practices in design and installation.

Batch evaporators

A batch evaporator consists of a vessel equipped with a heating jacket or internal coil, an overhead condenser, a condensate receiver, and usually, a source of vacuum. An example of a flowsheet for such an evaporator is shown in Figure 6. Feed is charged into the vessel, either by pumping, or more commonly, drawn in by vacuum. Heat is then applied and evaporated vapor is condensed overhead, while the contents of the vessel decrease in volume and increase in concentration of non-volatiles. Alternatively, in semi-continuous mode, additional feed is added through the feed-charging line as room allows. This way, at the end of the process, the vessel is full of product at the final concentration, rather than only partially full.

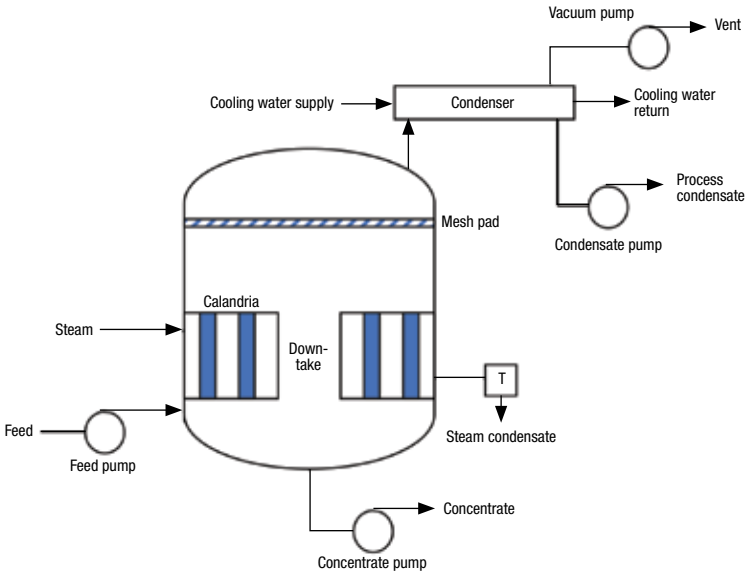

FIGURE 7. The short-tube vertical evaporator is one of the oldest designs still in common use

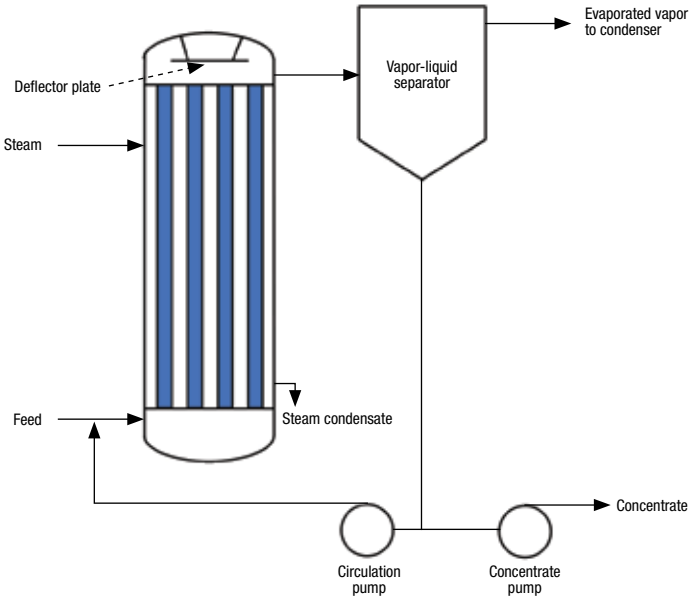

FIGURE 8. In this long-tube rising-film evaporator, a film forms on the inside of the tubes. Evaporation occurs as the film rises, and the generated vapor causes the film to thin and accelerate

The heat source is usually steam, but sometimes hot oil or another heat-transfer fluid is used. Cooling fluid may be applied to reduce the temperature of the final concentrate prior to unloading. While some cooling is usually necessary for personnel safety, concentrate is often removed at an elevated temperature to avoid high viscosity and to ensure that the fluid will drain completely or is pumpable. City, well or cooling-tower water is typically used, but chilled water or aqueous ethylene or propylene glycol are also options.

Usually, the vessel is equipped with a mixer, which provides several benefits. The mixer facilitates liquid motion at the heat-transfer surface, resulting in a higher heat-transfer coefficient. In addition, any solids present initially or generated during the concentration are kept in suspension. Gradients in temperature or concentration are mostly eliminated, which typically reduces bump-over and allows for a smoother process. For semi-continuous operation, the mixer ensures that the incoming feed is quickly blended into the contents of the vessel, avoiding cold spots. However, while usually preferred, a mixer is not always essential because considerable movement results from the boiling itself. Disadvantages are increased maintenance, the need to seal against vacuum and higher capital cost, not only for the mixer itself, but also for the increased structural strength of the vessel needed to support it.

In Figure 6, condensed vapor is directed into one of two receivers. At any given time, one receiver is in service while the other is standing by. When full, the in-service vessel is taken offline, while the standby unit is evacuated then brought online. Without prior evacuation, a disruption in system vacuum would occur upon opening the valve connecting the standby receiver to the condenser. The vessel should be evacuated using an auxiliary vacuum source, rather than the same one used to generate the system vacuum, also to avoid a bump in the system vacuum. Once the fresh vessel is in service, air (or an inert gas such as nitrogen) is introduced into the full one to break the vacuum, then the vessel is drained and put on standby. Alternatively, a single receiver and a pump can be used in place of the two receivers and an auxiliary vacuum source.

The main advantages of a batch evaporator are simplicity, flexibility, relatively low cost and the ability to handle feeds containing undissolved solids — for example, jams and jellies with whole fruit [*4*]. On the other hand, there are several disadvantages, including low heat-transfer coefficients, low heat-transfer area per unit vessel volume, and the inherent loss of productivity with batch versus continuous operation. In addition, because of the extended residence time, batch evaporators are not suitable for heat-sensitive products. In spite of these disadvantages, however, batch evaporators are often chosen for specialty operations that require the flexibility to handle small volumes of multiple products, when the volume of any single product is not sufficient to justify the use of a continuous evaporator. When possible, similar products are run consecutively, so that extensive cleaning between products may not be necessary.

FIGURE 9. Unlike its rising-film counterpart, this falling-film evaporator needs a distributor to ensure uniform distribution of liquid to each tube

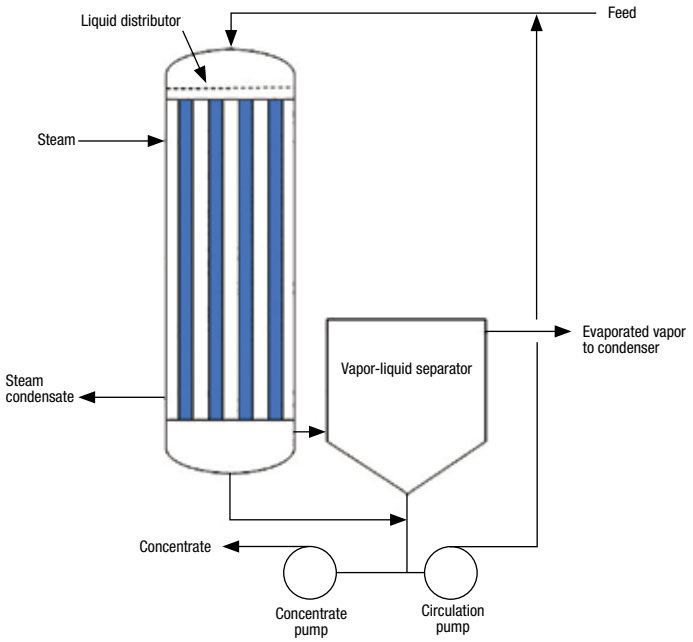

Short-tube vertical evaporators

The short-tube vertical evaporator, also known as a Roberts evaporator, is one of the oldest designs still in common use. The major application is concentration of sugarcane juice. In addition to their use as evaporators, these units are employed as evaporative crystallizers, primarily for the production of sugar.

A schematic representation of a short-tube vertical evaporator is shown in Figure 7. The shell-and-tube heat exchanger is situated inside of the evaporator vessel, near the bottom. As suggested by the name, the tubes are short relative to the height of the vessel. The heat exchanger, called the calandria, contains an open area at the center, known as the downtake. Process fluid circulates upward through the calandria tubes, against condensing steam on the shell side. The vapor formed travels to the top of the evaporator, where entrained liquid droplets coalesce on the mesh pad and fall back into the boiling liquid. Meanwhile, the liquid emerging from the calandria tubes travels downward through the downtake, then back up through the tubes for a subsequent pass.

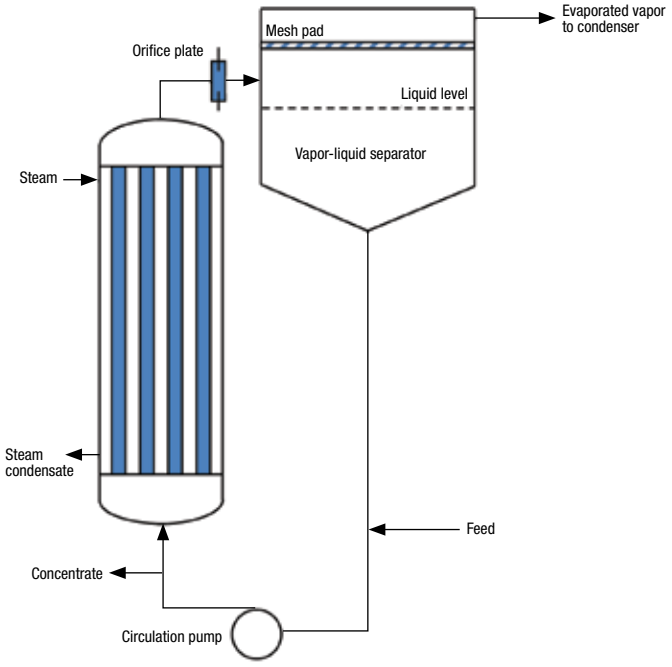

This circulation occurs by natural convection, as in a thermosyphon reboiler in a distillation column. That is, the lighter vapor-liquid mixture rises in the tubes as it is displaced by the heavier liquid coming from the down-

FIGURE 10. In this forced-circulation evaporator, boiling does not occur in the tubes. Instead, vapor forms as the superheated process material flashes across the orifice plate

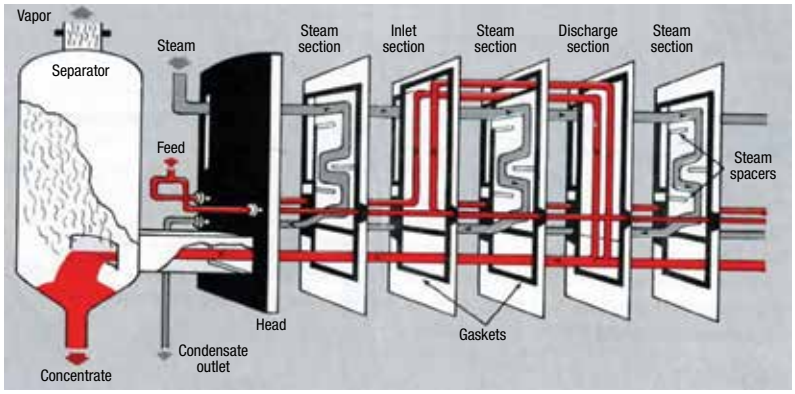

FIGURE 11. This rising-falling-film plate evaporator was first introduced in 1957, and is still in common use today [*4*]

take. As an alternative to the continuous operation depicted in Figure 7, these evaporators can be operated in batch mode, as is done in the sugar industry.

Why is the downtake needed? That is, why is it insufficient for the vapor-liquid mixture in the tubes simply to be replaced by the incoming feed? The reason is that the circulation rate is much higher than the feedrate, and without circulation, the linear velocity would be too low to obtain an adequate heat-transfer rate. To accommodate this relatively high circulation rate, the downtake area is about half that of the tubesheet. Typically, tubes are 2–3 in. in diameter by 4–6 ft in length, and the linear velocity through the tubes is about 3 ft/s. Generally, heat-transfer coefficients are highest when the liquid level, as indicated by an external sight glass, is about halfway up the tubes. Lower levels lead to incomplete wetting, and in turn, rapid fouling of the heat-transfer surface, a situation commonly known as burn-on. Higher levels are used for materials with a greater tendency to foul, or if the evaporator is also a crystallizer. A mixer is not needed, although the use of one can improve heat transfer, increasing capacity by as much as a factor of two. Use of a mixer may be preferred in crystallization service, not only for better heat transfer, but also to keep larger crystals from settling. However, there are many short-tube evaporator-crystallizers without mixers.

Short-tube vertical evaporators offer several advantages. Because the tubes are large in diameter and short in length, they are easily cleaned, and are well suited for materials that require mechanical descaling. Other advantages are low headroom requirement, proven designs based on many years of experience, and relatively low cost. Disadvantages include low heat-transfer coefficients, low heat-transfer area per unit volume, high floor-space requirement, large weight and high holdup of process material. In addition, use with corrosive materials is not advisable, because with the large evaporator body, a corrosion-resistant alloy would incur considerable cost.

Long-tube vertical-film evaporators

These evaporators operate with a thin film of liquid on the heat-transfer surface. As evaporation takes place, vapor fills the core of the flow channel, which thins and accelerates the film. The thin film and high fluid velocity lead to high heat-transfer coefficients, allowing a given evaporation capacity to be achieved with a relatively low ΔT. The low ΔT not only lowers the maximum temperature, but also reduces the occurrence of hot spots. Moreover, because the product exists as a thin film rather than filling the entire tube volume, liquid holdup, and in turn residence time, are low, minimizing heat exposure. Other advantages of film evaporators are low cost per unit area, simple construction, low floorspace requirement, ability to handle foamy liquids and ability to handle corrosive process streams.

Because of these advantages, film evaporators are preferred for many applications, and they represent more evaporation capacity than all other types combined. These evaporators are especially well suited for concentration of heat-sensitive materials, such as fruit and vegetable juices. On the other hand, some applications are not suitable — for example, high-viscosity fluids (>300–400 cP), because film formation is difficult. In addition, film evaporators are not recommended for materials with a high fouling tendency, or if solids are present or may form. These situations are usually handled with a forced circulation evaporator (discussed later).

A schematic drawing of a rising-film evaporator, the first film evaporator, is shown in Figure 8. Tubes are typically 1–2 in. in diameter, and their length ranges from less than 20 ft to more than 30 ft. Feed enters the bottom and is directed upward. Because the feed is usually subcooled, some portion of the heat-transfer area is needed to bring the temperature to the boiling point. Consequently, there is a hydrostatic head of liquid at the bottom of each tube that must be overcome. Afterward, the liquid film forms on the heat-transfer surface. The evaporated vapor accelerates the film, which becomes thinner as the two-phase mixture moves toward the top of the heat exchanger. Eventually, the high-velocity stream of vapor and concentrated

liquid emerges at the top, impinges on a deflector plate, and then enters the vapor-liquid separator. The vapor goes to the condenser, while the concentrated liquid is removed as product. The design shown in Figure 8 provides for a portion of the concentrate to be recycled. This is necessary when the ratio of feed to concentrate volume is high, to ensure that there is sufficient liquid to keep the tubes wet.

In a falling-film evaporator (Figure 9), the feed enters the top rather than the bottom of the heat exchanger. Unlike its rising-film counterpart, there is no static head of liquid caused by subcooled feed. Instead, assisted by gravity, the film forms immediately. Films are thinner and faster-moving than with the rising-film evaporator, leading to higher heat-transfer coefficients that make economic operation possible at ΔT values as low as 7°F. Moreover, the residence time is shorter than with rising-film units, typically only 15–30 s. This is attributable to the thinner film with the falling-film design, and also the absence of the column of liquid that occurs with rising-film units when the feed is subcooled.

For proper operation of a falling-film evaporator, the feed must be evenly distributed among the tubes. Tubes that receive insufficient feed may experience dry spots, localized overheating, increased fouling and reduced heat-transfer coefficients. Conversely, if too much liquid is delivered to a tube, film formation may be difficult, and the final concentration may be too low. To ensure adequate distribution, a distributor is placed over the top tubesheet. Perhaps the most common type is the orifice-type distributor, which is simply a metal plate with holes that direct the liquid flow. Another method is to use spray nozzles to direct liquid into each tube.

Forced-circulation evaporators

A schematic drawing of a forced-circulation evaporator is shown in Figure 10. Process fluid circulates from the vapor-liquid separator, also called the flash chamber, through the heat exchanger and back. The orifice plate (alternatively, a control valve or simply hydrostatic head may be used) applies enough back-pressure to prevent boiling in the heat exchanger. For this reason, this type of evaporator is also called a sup-

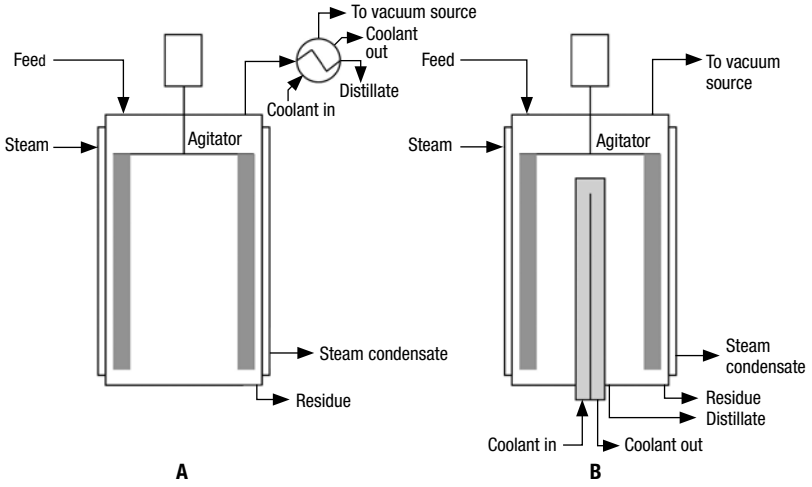

FIGURE 12. Agitated thin-film evaporators use a rotating blade to form a film on the heated surface. The condenser can be either external (A) or internal (B)

pressed boiling evaporator.

Only sensible heat (no latent heat) is transferred in the heat exchanger, and the process liquid exits the heat exchanger at a temperature above the boiling point at the prevailing pressure in the flash chamber. The pressure drop across the orifice (or other back-pressure device) leads to flashing as the liquid enters the flash chamber. The flashed vapor is directed to an overhead condenser, usually via a mesh pad to recover entrained liquid droplets. Meanwhile, the concentrated liquid makes another pass through the heat exchanger, with some new feed added, and some concentrate removed as product. The circulation rate is much higher than the feed and concentrate flowrates, as well as the evaporation rate. Typically, the circulation rate is 220–330 lb/h per 1 lb/h of evaporation [*4*], and the linear velocity in the heat-exchanger tubes is 6–15 ft/s.

Forced-circulation evaporators are less efficient than film evaporators. Heat-transfer coefficients are lower, meaning cost per unit heat-transfer area is higher. Cost is also driven up by the need for the large circulation pump and piping. The high linear velocity leads to high pumping and maintenance costs, and if abrasive solids are present, erosion problems. Moreover, the large flash chamber results in high process liquid holdup and residence time. Because of these disadvantages, a forced-circulation evaporator is chosen only when a film evaporator will not work. Such applications include viscous liquids, because these do not form a film easily. The forced-circulation design is also appropriate for products that have (or may have) crystals or other solids present, or are heavily fouling, because the high linear velocity keeps solids in suspension, hinders formation of a fouling layer and prevents plugging.

Plate evaporators

Although the discussion so far has focused primarily on tubular evaporators, flat plates are also used as the heat-transfer surface. A plate heat exchanger comprises a series of corrugated metal plates, separated by polymeric gaskets around the periphery of each plate. The plates are attached to a frame, then pressed together to form a series of flow channels. Steam and process fluid are directed to alternate channels, and heat is transferred across each plate from the steam side to the process side. Orifices, slotted openings and elastomeric seals are located to direct the various streams where they need to go, and to exclude them from places they do not belong. Baffles are employed to create a tortuous flow path for the process fluid that increases local velocity, and in turn, heat-transfer efficiency. Plate spacing is typically ¼ to ½ in. The corrugations allow the plates to contact each other at a number of points so that distortion is minimized. As with tubular evaporators, both film and forced-circulation designs are available, and the selection criteria are the same.

The rising-falling-film plate evaporator, developed by APV (now part of SPX Flow) in 1957, was the original plate evaporator, and is still in common use today. As shown in Figure 11, every other product channel is a rising pass, and the alternate product channels are falling passes. Feed, delivered through two parallel ports, is equally distributed to each of the rising-film passageways. The feed temperature is slightly higher than the saturation temperature. The resulting flash promotes turbulence, leading to more uniform distribution and better heat transfer. The liquid-vapor mixture rises to the top of the rising pass, then moves through a slot in the adjacent steam plate to the falling pass. There, gravity further assists film movement as the evaporation process is completed. In both the rising and falling passes, rapid movement of the thin film leads to low residence time and a high heat-transfer coefficient. The mixture of vapor and concentrate from all falling passageways flows through a rectangular duct to the vapor-liquid separator [*4*].

Plate evaporators offer several advantages over tubular designs in certain applications. The corrugations and the tortuous flow path lead to turbulent flow at Reynolds numbers as low as 100 to 400. The resulting high heat-transfer coefficients allow a given evaporation rate to be reached at a lower ΔT. This, along with the low holdup and short residence time, make the plate evaporator a good choice for heat-sensitive products. In addition to improved heat transfer, the high fluid velocity results in a lower rate of fouling when compared to tubular evaporators. Plate packs are easily disassembled for inspection and cleaning, hence the popularity of plate evaporators in food applications. Other advantages are the ability to add plates for additional capacity (limited by the size of the frame), low headroom and no need for supporting steelwork because the units are self-supporting.

A disadvantage of plate evaporators is the propensity to allow air leakage at higher temperatures. In addition, plate evaporators are not economical for high capacities. In general, rising-falling-film designs are suitable for water removal rates up to about 35,000 lb/h, while falling-film units, which have larger vapor ports, can handle up to 60,000 lb/h [*4*]. In plate evaporators, the maximum allowable pressure difference between the steam and process sides is about one bar, which may not provide adequate ΔT if boiling point elevation is high. Finally, materials of construction are limited — for example, unlike tubular evaporators, graphite is not used.

Agitated thin-film evaporators

Unlike the film evaporators discussed above, agitated thin-film evaporators form the film mechanically, using a rotating blade situated near, or even contacting, the heat-transfer surface. As shown in Figure 12, the device comprises a mechanical rotor situated concentric to a cylindrical, jacketed body. Feed entering the top of the evaporator is distributed evenly by the rotor, then the process fluid spirals down the heated wall. Bow waves developed by the rotor blades, named for the waves that form at the bow of a ship as it moves through the water, generate high turbulence [*5*]. Consequently, heat-transfer coefficients are high, and volatile compounds evaporate rapidly.

Concentrate, usually called residue when referring to agitated thin-film evaporators (TFEs), exits the bottom, with flow of evaporated solvent either cocurrent or countercurrent. With the latter, vapor exits the top and proceeds to an external condenser, a setup that is called a wiped-film evaporator (WFE). For cocurrent flow, vapor travels from the heated surface to an internal condenser, situated concentric to the evaporator body, and the resulting condensate (usually called distillate) proceeds downward to its own exit at the bottom. Because the evaporator and condenser surfaces are physically close, this arrangement is known as a short-path evaporator or short-path still, and the evaporation process is called short-path distillation.

Unlike the other types of evaporators discussed in this article, the agitated TFE is typically used with organic rather than aqueous systems. Usually (but not always) the distillate is the product. Most rotors have a fixed clearance between the outer edge and the body wall, ranging from 1.25 mm for small evaporators up to 5 mm for large ones. Alternatively, the edge of the rotor can be fitted with an elastomeric material that actually touches the wall, but this is less common. Rotational speed may be as high as 40 ft/s, with the power requirement ranging from 0.25 to 2.5 hp per ft^2 of heat-transfer area. Units with up to 160 ft^2 of heat-transfer area are standard. The heat source is usually steam or hot oil, although smaller units are electrically heated [*3*, *5*].

Agitated TFEs offer several advantages. Residence time is short (as low as a few seconds), and because the rotor action provides close to plug flow with little backmixing, the residence-time distribution is narrow. Surface renewal is rapid, which minimizes fouling, and holdup is low. Turbulence in the agitated film leads to high heat-transfer coefficients, which partially offset the considerable cost per unit heat-transfer area. High ratios of feed to residue flow are possible without circulation. The mechanical action allows thin-film units to handle feeds with viscosities up to 50,000 cP, or even higher with specialized designs.

Short-path units can be operated at very high vacuum, by virtue of the internal condenser. Because the distance traveled by the evaporated vapor is short, pressure drop is exceedingly low. Consequently, absolute pressures as low as 0.01 mm Hg are obtainable with a conventional vacuum pump, or even lower if a diffusion pump is included. Conversely, units with an external condenser incur a higher pressure drop between the evaporator body and the condenser. The achievable evaporation pressure is about 1 mm Hg, which is lower than most conventional evaporation and distillation systems, although not as low as with the short-path design. If lower pressure is not needed, an external condenser may be preferred because the simpler construction results in a lower cost, and the capacity limitation from the relatively low surface area of an internal condenser is avoided.

The high vacuum possible with a short-path unit allows recovery of heavy compounds with minimal heat damage, because boiling points are lower. The technique is often used to process residues obtained from conventional distillation processes, which do not operate at the low pressures achievable in short-path distillation. At the highest practical bottoms temperature, the residue from a conventional column may still contain significant levels of valuable low-volatility components. These can be recovered at a lower temperature in a short-path still, without thermal degradation. Moreover, such feeds are often highly viscous, and would be difficult to process without mechanical film formation. Such viscous materials usually require heat tracing on the piping, especially the residue, but also the feed, to avoid excessive viscosity. Even the distillate pipe may require heat tracing to keep the viscosity down, prevent precipitation or stay above the melting point. In some applications, such problems are avoided by using heated fluid on the condenser, rather than cold fluid as with conventional evaporators.

In summary, the low operating pressure, short residence time, low holdup and wiping action make agitated TFEs well suited for heat-sensitive, viscous, fouling or high-boiling liquids. Disadvantages are the increased complexity and maintenance incurred by the rotor, inability to handle particulate matter and costs that are 20 to 30 times higher than tubular evaporators of similar capacity. ■

Edited by Mary Page Bailey

References

1. Perry, R.H., Green, D.W., Maloney, J.O., eds., "Perry's Chemical Engineers' Handbook," 7th ed., McGraw-Hill, New York, Section 11, 1997.
2. Prost, J.S., González, M.T., Urbicain, M.J., Determination and correlation of heat transfer coefficients in a falling film evaporator, *J. Food Engr.,* 73 (2006), pp. 320–326.
3. McCabe, W.L., Smith, J.C., Harriott, P., "Unit Operations of Chemical Engineering," 7th ed., McGraw-Hill, New York, 2005.
4. APV Evaporator Handbook, SPX Flow, Inc., 2009.
5. Glover, W.B., Hyde, W.L., Evaporation of Difficult Products, *Chem. Proc.*, February 1997.

Author

Alan Gabelman is president of Gabelman Process Solutions, LLC (6548 Meadowbrook Court, West Chester, OH 45069; Phone: 513-919-6797; Email: alan.gabelman@gabelmanps.com; Website: www.gabelmanps.com), offering consulting services in process engineering. Gabelman's over 40 years of experience include numerous separation processes and other engineering unit operations, equipment selection, sizing and design, process simulation, P&ID development, and process economics. He holds B.S., M.Ch.E. and Ph.D. degrees in chemical engineering from Cornell University, the University of Delaware and the University of Cincinnati, respectively. He is a licensed Professional Engineer and has served as an adjunct instructor in chemical engineering at the University of Cincinnati. Gabelman has edited a book on bioprocess flavor production, and he has authored several technical articles and a book chapter.

Sampling System Design: Managing System Variables

Understanding the effect of flowrate, velocity, density, viscosity, pressure drop, friction, components and sample line sizes will help you design a sampling system

Randy Rieken
Swagelok Company

IN BRIEF

Credit 1b and 1d: Swagelok

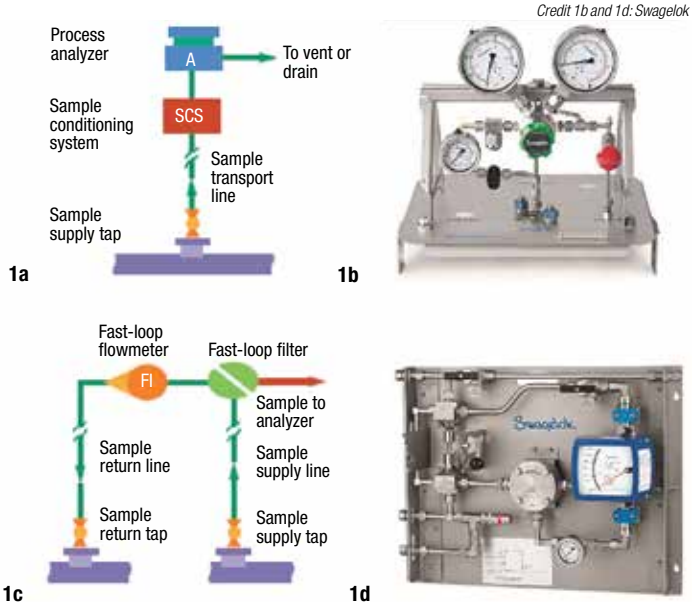

FIGURE 1. Minimizing the amount of material sampled reduces waste and limits disruptions to the process stream. Reducing the flowrate through a single-line sampling system (1a and 1b), which disposes of samples via a vent, flare, or drain, will reduce process fluid waste. Reducing the flowrate through a fast-loop system (1c and 1d) that returns the sample to process will reduce the potential for interference with the process stream (Source: 1a and 1c from Ref. 1)

The primary goal when designing an analytical sampling system is to ensure timely, accurate measurements. The sooner you can discover anomalies in a process stream, the sooner you can react to correct them. To meet this goal, your sampling system should minimize time delay, or the total time elapsed from tapping the process stream to completing sample analysis. It should also ensure that the sample is not contaminated and accurately represents true process-stream conditions. This may require some form of conditioning, such as maintaining sample temperature, as the sample moves from the process tap to the analyzer.

An additional consideration is to minimize the amount of material sampled to reduce waste and not disrupt the process stream. If the sampling system is a single-line setup that disposes of sample material via a vent, flare, or drain (Figures 1a and 1b), you should minimize the flowrate to avoid wasting an excessive amount of process fluid. If it's a fast-loop system that returns the sample to process (Figures 1c and 1d), make sure the flowrate isn't so high that it interferes with the process stream.

To achieve the above guidelines, you'll need to experiment with and refine multiple variables related to your system layout and performance, including the following:

Type of flow. Turbulent flow is typically preferred over laminar flow in a sampling system to ensure the sample is properly mixed. A parameter known as the Reynolds number (Re) will help you determine whether the flow is laminar or turbulent and to what degree.

Fluid properties. The fluid's velocity, density, and viscosity are all variables that are included in the Re equation. These variables can be manipulated in some manner in an effort to achieve turbulent flow.

Pressure differential. The pressure drop between the process tap and the return

TABLE 1. REYNOLDS NUMBER (*RE*) FOR TYPICAL LINE CONDITIONS					
ρ/η Ratio s/m^2	Tube 1/4 in. × 0.035 in.	Tube 3/8 in. × 0.035 in.	Tube 1/2 in. × 0.049 in.	Pipe 1/2 in. SCH80	Pipe 3/4 in. SCH40
1×10^5	457	775	1,020	1,390	2,090
2×10^5	914	1,550	2,040	2,770	4,190
3×10^5	1,370	2,320	3,060	4,160	6,280
4×10^5	1,830	3,100	4,080	5,550	8,370
5×10^5	2,290	3,870	5,110	6,940	10,500
7×10^5	3,200	5,420	7,150	9,710	14,700
1×10^6	4,570	7,750	10,200	13,900	20,900

Re for a fluid velocity of 1 m/s (Re doubles at 2 m/s)
For gas samples, the ρ/η ratio increases in proportion to absolute pressure

Laminar Flow | Critical Zone | Turbulent Flow

Source: "Industrial Sampling Systems" [*1*]

point in a fast-loop system must be sufficient to drive the desired flow through the lines. The Darcy equation will help you determine the pressure loss and whether you need to adjust flow velocity or line diameter.

Friction factor. Sampling lines with a lower friction factor help to reduce pressure drop. System operating conditions influence the friction factor, and it will need to be recalculated with any system changes.

Bends, fittings and components. Longer sampling systems experience lower velocities and greater pressure drops. Simply reducing their overall length, including the number of bends, could yield the desired performance for a system. When determining a system's actual length, include the sampling lines, as well as the equivalent lengths of all the components. Equivalent lengths represent the internal flow paths of elbows, tees, valves, returns and more converted into the length of a straight tube or pipe to account for the resistance of the entire flow path.

Diameter of sampling lines. The right sampling line size depends on your target response time and the available source pressure. Sometimes adjusting both supply line and return line sizes will help; other times changing just one line will be the right choice.

Based on the above variables, your system design process will take some trial and error. First, gather all known information about the system, and then try manipulating different variables to determine if you can achieve your desired performance.

Note that these variables are highly interrelated. A single adjustment may require complete reworking of your calculations. This article will help give you a better understanding of how these variables are correlated. In addition, it includes a comprehensive design example for a fast-loop sampling system (see sidebar on p. 41), which demonstrates how modifying just one variable can help you achieve the desired time delay, accuracy, and flowrate for your sampling system.

Fluid velocity in the line

Start by deciding the velocity you need. This is a fundamental design objective. Usually, it's sufficient to simply divide the sample line length in meters by the transport time desired, t.

$$u = L/t \qquad (1)$$

Where:
u = Fluid velocity, m/s
L = Line length, m
t = Desired transport time, s

For example, if the sample line is 100 m long and you want to limit the delay to one minute, the required velocity is $u = L/t$ =100 m/60 s = 1.7 m/s.

If possible, ensure that the velocity is greater than 1 m/s, as this will help to keep the lines clean. A velocity of 1–3 m/s is recommended for liquids and 2–5 m/s for gases.

Turbulent or laminar flow

The flow within the lines of your analytical sampling system will have one of two types of patterns — laminar or turbulent (Figure 2). Each type is highly dependent on the velocity of the sample fluid, as well as the density and viscosity of the fluid.

Source: Ref. 1

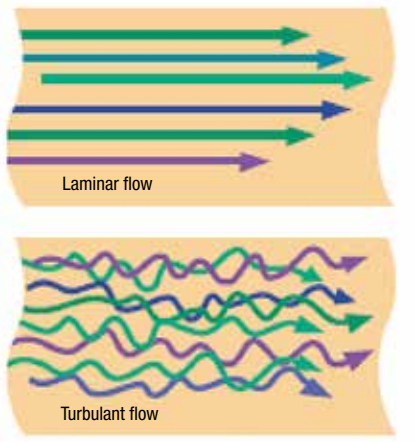

FIGURE 2. In laminar flow (top), which occurs when the sample velocity is low, fluid movement is parallel to the sample lines. In turbulent flow (bottom), which occurs at higher velocities, fluid moves randomly across the line, encouraging good sample mixing. In addition to fluid velocity, the type of flow is also dependent on the fluid's density and viscosity

Turbulent flow is typically preferred, as it enables faster analyzer responses and minimizes the settling of solids in sample lines to avoid contamination and clogging. However, turbulent flow isn't always achievable. Sometimes you'll have to accept the inherent deficiencies of laminar flow, including slower analysis.

Evaluating the Reynolds number (Re) is an easy way to determine the type of flow. This value provides a relative marker of the flow type and the degree to which it is laminar or turbulent. An Re value less than 2,000 typically indicates laminar flow. And an Re value of 4,000 or more indicates turbulence. However, turbulence usually begins before the Re reaches 4,000, but only to a degree. Therefore, you can't accurately define the type of flow if your Re is in the critical zone between 2,000 and 4,000.

The Reynolds number (Re) can be calculated using Equation (2):

$$\mathrm{Re} = \frac{D' \cdot \rho \cdot u}{\eta'} \qquad (2)$$

Where:
D' = Line internal diameter, mm
ρ = Fluid density, kg/m^3

DESIGN EXAMPLE: OPTIMIZING A FAST-LOOP SAMPLING SYSTEM

With a better understanding of the variables involved when designing an analytical sampling system, let's walk through the design process and learn how some fine-tuning can optimize the performance of your system.

The following example describes a fast-loop sampling system that transports a pure water sample to a silica analyzer. A small portion of the flow passes through the analyzer, and most of the flow returns to the process.

Here are some specifics about the system:

- Supply line: 60 m
- Return line: 120 m
- Operating conditions: ambient
- Sample transport time (time delay): must not exceed 1 minute
- Pressure differential: 5 bars from the supply tap to the return tap
- Elbow fittings: 10 in. each line

Solving by trial and error

With the transport line at ambient conditions, fluctuating outside air temperature and pressure may affect system conditions. Therefore, you'll need to consider the worst-case conditions for the process fluid's viscosity and density.

The viscosity of water increases at low temperatures (see Table 2). Its highest viscosity (η') is 1.80 cP at 0°C. And water's highest density (ρ) occurs at 4°C when it reaches 1,000 kg/m^3. If the fast-loop design works under these viscosity and density conditions, it will work at any ambient temperature.

Next, consider the fluid velocity (u). The recommended design velocity for high-purity water samples is 2 m/s, which will transport the sample 60 m in 30 s.

Choose a line size arbitrarily, and determine the pressure drop (ΔP'). For starters, let's try ½-in. × 0.049-in. wall tubing, which has an inside diameter (D'), or bore, of 10.2 mm.

Don't forget to add the equivalent length of the 10 elbow fittings to account for the additional pressure drop. From Table 4, the equivalent length of a tube elbow is 60 times the inside diameter of the line. Therefore, the effective length of the two lines is 66 m (supply line) and 126 m (return line), or 192 m total:

L_1 = 60 m + (10 × 60 × 0.010) m = 66 m

L_2 = 120 m + (10 × 60 × 0.010) m = 126 m

L = 66 m + 126 m = 192 m

To determine whether the sampling system flow is turbulent or laminar, calculate the Reynolds number using Equation (2):

Re = (10.2 × 1,000 × 2.0)/1.8 =1.8 = 11,000. At 11,000, the flow is turbulent.

From Equation (5), the relative roughness is ε'/D' = 0.0015/10.2 = 0.00015. This value returns a friction factor (f) of 0.031 from the Moody chart (Figure 3).

Now, determine the pressure drop for the complete fast loop using Equation (4):

$\Delta P' = (0.031 \times 192 \times 1{,}000 \times 2.0^2)/(2 \times 10.2)$ = 1,200 kPa

The pressure loss is 12 bars, which is more than twice the available pressure differential of 5 bars. Therefore, the ½-in. tubing will not work. It needs to be larger. Performing calculations reveals that 1-in. × 0.083-in. wall tubing is just large enough, yielding a pressure drop of 450 kPa. However, note that the flowrate with this size tubing will be 42 L/min, which is quite high and will lead to more expensive flowmeters, tubing, valves and fittings.

Many system designers may stop here, having achieved an adequate pressure differential, despite the high flowrate. But you can improve these results with a simple design adjustment — using a larger tube only in the return line.

Perfecting the design

Keeping the ½-in. tube for the supply line, its effective length is 66 m; so its pressure drop is:

$\Delta P' = (0.031 \times 66 \times 1{,}000 \times 2.0^2)/(2 \times 10.2)$ = 400 kPa

With the supply line pressure dropping by 4 bars, only 1 bar is left for the return line, which is twice as long. This remaining pressure may appear to be inadequate to return the sample to process. However, remember that fluid velocity drops when flow enters a wider bore, which substantially reduces the rate of pressure loss.

For the return line, consider using larger tubing with a ¾-in. outside diameter x 0.049-in. wall, which has a bore of 16.6 mm. With a velocity of 2.0 m/s in the supply line, the new return line velocity is 0.76 m/s, computed as follows:

$u_2/u_1 = (D_1/D_2)^2$

$u_2 = 2.0 \times (10.2/16.6)^2 = 0.76$ m/s

Double-checking the type of return flow shows that it is still turbulent, with a Reynolds Number of 7,000:

Re = (16.6 × 1,000 × 0.76)/1.8 = 7,000

Calculate the relative roughness of the tubing, and look up its friction factor:

ε'/D' = 0.0015/16.6 = 0.00009

f = 0.034

The effective length of the return line, including the equivalent length of the 10 larger elbows, is now 130 m:

L_2 = 120 m + (10 × 60 × 0.0166) m = 130 m

The pressure loss in the return line is

$\Delta P' = (0.034 \times 130 \times 1{,}000 \times 0.76^2)/(2 \times 16.6)$ = 77 kPa

The total pressure drop is now 4.8 bars — 4 bars for the supply line and 0.8 bar for the return line, which satisfies the constraints of the system.

To find the necessary volumetric flowrate (dV/dt), multiply the velocity (u) in one of the lines by the unit volume (V_0) of that line:

$dV/dt = u \cdot V_0$

The supply line runs at a velocity of 2 m/s. The unit volume of the ¾-in. outer diameter x 0.049-in. wall tubing is 0.082 L/m. Therefore, you'll need to set the flowrate at 10 L/min:

dV/dt = 2.0 m/s × 0.082 L/m × 60 s/min = 9.8 L/min

The new design, using ½-in. tubing for the supply line and ¾-in. tubing for the return line, is less expensive to install compared to using 1-in. tubing for both lines; yet it delivers the same performance. In addition, this design will have less impact on the process because it draws only 10 L/min instead of the 42 L/min required by the larger line.

A refined solution

As demonstrated above, the best design solution went beyond the quick fix of 1-in. tubing for the entire sampling line. By taking the time to calculate a different scenario, we have reduced the cost of the system and minimized its flowrate. It may be possible to achieve even better results by fine-tuning additional variables, but for now, this solution is certainly acceptable. ❐

u = Fluid velocity, m/s

η' = Fluid viscosity, cP

To achieve a suitable turbulent flow, you may need to adjust some system variables, including the internal diameter of sample lines and the fluid velocity. Table 1 demonstrates how the Re value increases as line size increases. In addition, you can sometimes manipulate the density and viscosity of the fluid by adjusting the pressure and temperature of the sample lines.

It helps to know the density-to-viscosity ratio (ρ/η) of the sample fluid. Generally, a higher ρ/η ratio favors turbulence (see Tables 1 and 2). Application conditions may have an effect on the ρ/η ratio, so it's good to know how pressure and temperature influence the ratio — and there-

Source: Ref. 1

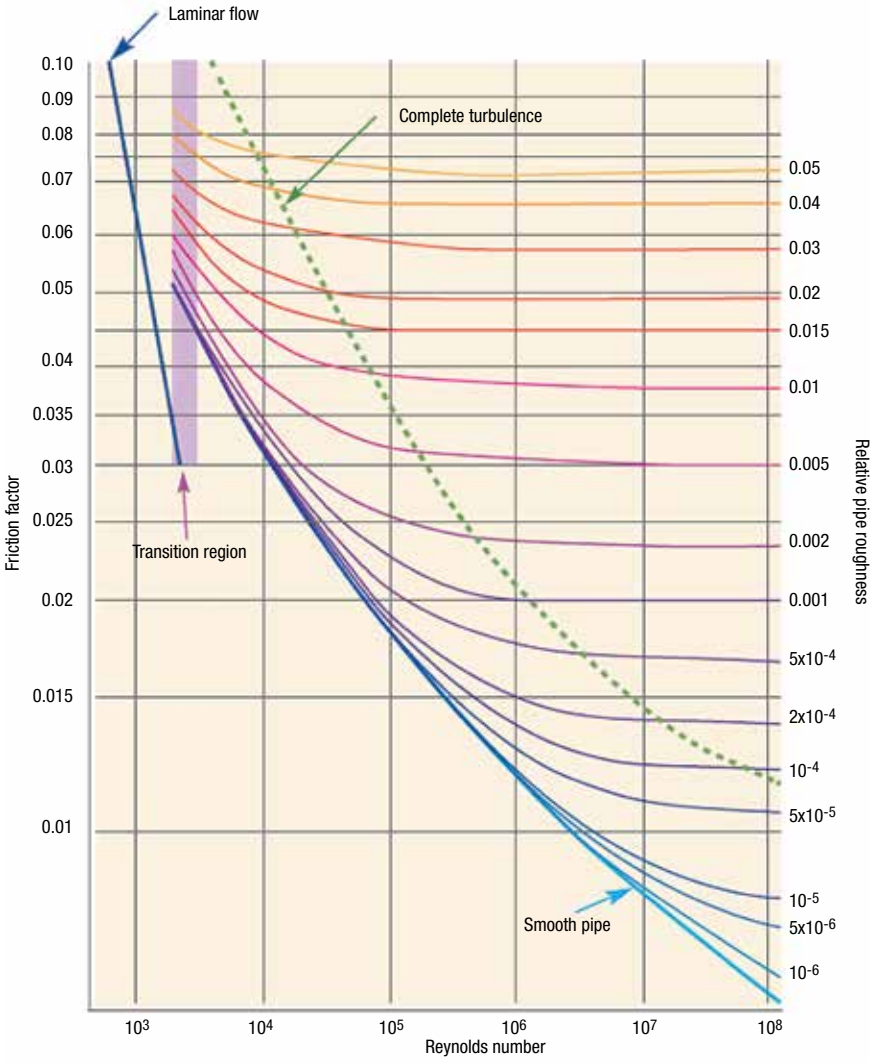

FIGURE 3. The Moody Friction Factor Chart provides friction factors (*f*) for sampling lines based on the Reynolds number (Re) of the system and the relative roughness (ε'/D') of the inside walls of the lines. The friction factor decreases as the Re increases, indicating less flow resistance and less pressure drop at higher Re values

fore turbulence — for both liquids and gases.

Liquids. For liquid samples, pressure changes will barely affect density or viscosity, and therefore system turbulence. However, temperature changes can influence the ρ/η ratio, as higher temperatures reduce viscosity, which increases flow and potentially turbulence.

Gases. For gas samples, increased line pressure has no effect on viscosity, but it compresses the gas, thereby increasing its density and the ρ/η ratio, favoring turbulence. And while increased temperature reduces the density of gas samples and increases their viscosity, the net effect is relatively small. Line temperature is usually set to avoid condensation without worrying about its effect on turbulence.

Calculating pressure drop

A sampling system must have enough of a pressure differential between the process tap and the return point to drive the desired flow through the lines to achieve the desired response time. If not, you'll have to modify the design, perhaps by using a larger return line.

Pressure will drop naturally within the sampling system due to a variety of factors, including line length and diameter, the number of bends in a system, elevation changes, friction, sample fluid density, and flow velocity. The system must be designed so it performs as desired when operating with the pressure differential actually available in the plant. To ensure this happy result, compute the expected pressure loss in your system design using the Darcy equation.

$$\Delta P = \frac{f \cdot L \cdot \rho \cdot u^2}{2D} \quad (3)$$

Where:
ΔP = Change in pressure, Pa
f = Friction factor
L = Line length, m
ρ = Fluid density, kg/m^3
u = Flow velocity, m/s
D = Line internal diameter, m

Entering all values in coherent SI units yields a ΔP value in Pascals. Alternatively, you can use millimeters for the line diameter (D') to determine the pressure drop ($\Delta P'$) in kiloPascals:

$$\Delta P' = \frac{f \cdot L \cdot \rho \cdot u^2}{2D'} \quad (4)$$

When making any adjustments to your system, your design work will focus on the flow velocity (u) and the line diameter (D), as application conditions fix the other variables.

The friction factor

When using the Darcy equation (Equation (3)), remember that the friction factor (f) is not a constant. This measure of the effect of friction on the walls of the sample lines varies with operating conditions.

As a resource, Table 3 provides friction factors for the limited range of tube and pipe sizes commonly used for sample lines. For tubes and pipes not shown, you can retrieve a friction factor from the Moody chart shown in Figure 3. To look up a value, you need to know the Re of the system and the relative roughness (ε'/D') of the inside walls of the sample lines. Notice that the friction factor decreases as the Re increases, indicating that there's less resistance to flow — and therefore less pressure drop — at higher Re values, assuming other variables remain constant.

The relative roughness of the tube or pipe is the ratio of absolute roughness (ε) to its internal diameter (D):

$$Relative\ roughness = \frac{\varepsilon}{D} \quad (5)$$

It is convenient to enter the values

TABLE 2. DENSITY AND VISCOSITY VS. TEMPERATURE

Fluid	Temp (T) °C	Density (ρ at 2 bara) kg/m^3	Viscosity (η) Pa·s	Ratio (ρ/η) s/m^2	Re†
Air	0	2.55	1.74×10^{-5}	1.47×10^{5}	670
	25	2.34	1.86×10^{-5}	1.26×10^{5}	580
	50	2.16	1.98×10^{-5}	1.09×10^{5}	500
	100	1.87	2.21×10^{-5}	8.46×10^{4}	490
Water	0	1,000	1.79×10^{-3}	5.57×10^{5}	5,700
	25	997	8.94×10^{-4}	1.12×10^{6}	11,000
	50	988	5.49×10^{-4}	1.80×10^{6}	18,000
	100	958	2.82×10^{-4}	3.40×10^{6}	35,000

† For air flowing in 1/4 in. × 0.035 in. tubing at 2 bara with a velocity of 1 m/s
† For water flowing in 1/2 in. × 0.049 in. tubing with a velocity of 1 m/s
Source: "Industrial Sampling Systems" [*1*]

TABLE 3. TURBULENT FRICTION FACTORS (MOODY)

Line size	1/4 in. tube 0.035 in. w	1/2 in. tube 0.049 in. w	1/2 in. pipe SCH40
Re	**Friction factor (*f*) if turbulent flow**		
10^6	0.016	0.014	0.026
10^5	0.020	0.019	0.027
50,000	0.022	0.021	0.028
10,000	0.031	0.031	0.035
8,000	0.033	0.033	0.037
6,000	0.036	0.036	0.039
4,000	0.041	0.041	0.045
3,000	0.044	0.044	0.046
Re	**Friction factor (*f*) if laminar flow**		
3,000	0.021	0.021	0.021
2,000	0.032	0.032	0.032

Source: "Industrial Sampling Systems" [*1*]

of ε and D in millimeters.

The absolute roughness is the actual wall irregularity of the tube or pipe, and it doesn't change much with diameter — typically 0.0015 mm for tubing and 0.05 mm for pipe.

Once you determine the Re and the relative roughness, estimate the friction factor from the Moody chart. The pressure drop is directly dependent on this value. Insert your number into the Darcy equation and figure the pressure loss in your line.

Allowing for bends

The number of bends in a sampling system contributes to pressure drop. Each sharp bend adds length (L), causing some additional pressure loss that you'll need to account for in your calculations. When possible, install lines with gradual bends, as the minimal additional length will barely affect the pressure drop. If this is impractical and you must use elbows — whether fittings or bent tubing — assign an equivalent length to each bend to account for the pressure drop it causes.

Table 4 lists some typical equivalent lengths expressed as multiples of the internal diameter. Multiply the appropriate length-to-diameter (L/D) value by your line bore to get the

Avoiding SIL Misconceptions

Engineers must refine their foundational understanding of process safety in order to avoid common misconceptions about safety instrumented systems, including safety integrity level (SIL) definitions

Afton Coleman
Emerson

Learnings from major industrial process accidents occurring over the past half century have driven awareness of functional safety and resulted in the development of two performance-based standards for manufacturers in the chemical process industries (CPI). These standards, introduced by the International Electrotechnical Commission (IEC; Geneva, Switzerland; www.iec.ch), are known as IEC 61508 and 61511.

A safety integrity level (SIL) is utilized as a measurement of required risk-reduction targets, as well as a way to represent achieved risk reduction. Although the functional safety standards have been in existence for many years, there are many common misconceptions around industry standards, as well as around the concept of SILs themselves.

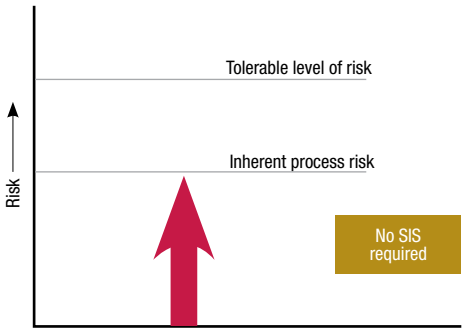

FIGURE 1. Low-risk case: In this case, the inherent process risk is lower than the operator's tolerable level of risk. Thus, no additional risk reduction is required

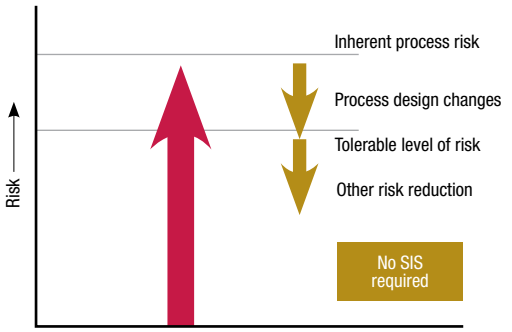

FIGURE 2. Moderate-risk case: Here, the inherent process risk is greater than the operator's tolerable level of risk, so risk reduction is required and met via means other than a safety instrumented system

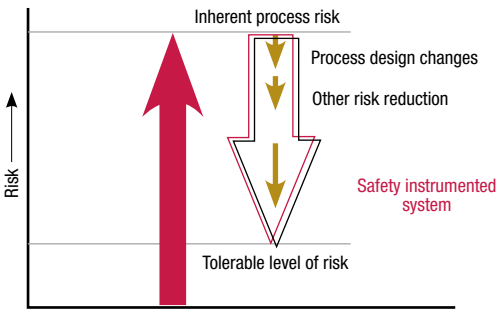

FIGURE 3. High-risk case: The inherent process risk is much greater than the operator's tolerable level of risk. Thus, risk reduction means, which may include design changes and other layers of protection, are implemented in addition to a safety instrumented system

Introduction to functional safety

Safety, in its most basic form, can be defined as freedom from unacceptable risk. Risk is a function of the likelihood of an incident occurring combined with its resulting consequence — specifically, a personal injury, loss of life or damage to the environment and equipment. The higher the likelihood and consequence, the higher the risk involved.

Functional safety is a part of the overall safety that depends on a system or equipment actively and correctly operating in response to its inputs to minimize risk. Safety instrumented systems (SIS) provide an active means of supporting functional safety, with a sensor to detect a dangerous condition and a logic solver to evaluate scenarios and activate a final element to respond and mitigate or reduce the consequence of the hazardous event. Such systems are commonly used in the CPI in accordance with IEC 61511 and 61508. A simple application example could be protection against vessel overpressure via a safety instrumented function (SIF). This would include pressure sensors set to detect high pressures within a vessel and the logic solver to determine whether the pressure within the vessel has become too high, in which case a final element is activated to open, relieving vessel pressure.

SIL and risk reduction

The functional safety standards IEC 61508 and 61511 have defined the measurement of performance required for a SIF. These standards provide guidance on how to specify a target level of risk reduction, as well as how to scrutinize the relative level of risk reduction provided by a SIF, to bring risk down to a tolerable level.

Initially, risk is measured by how likely it is that a given event will occur and how severe it would be; in other words: how much harm could it cause? There are different tools to quantify risk that are available to engineers, including the hazard and operability study (HAZOP), process hazard analysis (PHA) and so on. After the hazard's risk is quantified, it is compared with the end user's tolerance for risk. If the level of risk is greater than the tolerable level of risk, reduction measures are identified and evaluated to determine if risk can be reduced to an acceptable level. Often, active measures, such as basic process control system

FIGURE 4. Common elements within a safety instrumented function (SIF) include sensors, actuators, safety relays, programmable logic controllers (PLCs) and more

(BPCS) alarms or operator intervention, provide adequate levels of risk reduction. If so, a SIS is not required. However, if risk reduction must be reduced by a factor of greater than 10 (a risk-reduction factor, or RRF >10), a SIS should be used, or the process should be redesigned to reduce inherent risk further. Figures 1, 2 and 3 illustrate risk levels and potential system requirements for low-, medium- and high-risk cases.

Safety instrumented systems consist of one or multiple SIFs that address particular hazards. A SIF within a SIS consists of one or more sensors, logic solvers and final elements designed to actively detect and respond to a potentially dangerous condition, thus mitigating or reducing the consequence of the hazardous event (Figure 4). Common CPI applications include emergency shutdown, blowdown, vents to flare and so on.

IEC 61508 and 61511 set out the requirements for ensuring that systems are designed, implemented, operated and maintained to the required SIL. Four SILs are defined according to the risks involved in the application, with increasing risk reduction required by increasing SIL, as shown in Table 1.

Challenges and misconceptions

Electrical, electronic or programmable electronic systems (E/E/PE) can carry out a multitude of safety functions. The challenge is to design safety systems in such a way as to prevent dangerous failures or to control them when they arise. However, during the design phase, much of the focus has become around the selection of hardware with failure rates that meet a target SIL. This has led to some common misconceptions around the proper application of the functional safety standards and SIL in the CPI. Some of these misconceptions are described in the following sections.

Misconception: The IEC 61511 and 61508 standards will direct exactly how to design, install and operate a safe process. IEC functional safety standards are performance-based, not prescriptive. This means that they do not specify process design conditions or acceptable materials of construction, recommended operating conditions, or predetermine protective functionality. Instead, the standards publish the framework for manufacturers (IEC 61508) and process industries (IEC 61511) that defines a safety lifecycle approach to safety systems covering the analysis, design, implementation, operation and decommissioning of a SIS.

For example, end users are required to determine their tolerable level of risk reduction and design a process with the appropriate rigors, processes and competencies to ensure that systematic and random failure modes are minimized.

Misconception: Using a SIL-2-capable device (such as a transmitter or final element) is all that is needed to comply with functional safety standards. Safety integrity levels apply to the entire SIF loop, which consists of sensors, logic solvers and final elements. The SIL achieved is a function of the average probability of failure upon demand (PFD_{avg}) of the combined SIF devices, as well as the systematic integrity of each device.

For example, if there is a SIF consisting of the following elements: logic solver (SIL 3 capable) + sensor (SIL 2 capable) + final element (SIL 1 capable), the maximum SIL capability achievable is SIL 1, regardless of PFD_{avg} achieved.

Misconception: If all the products specified are SIL 3 certified products, the SIL 3 target is met. Device certificates are an indication of SIL capability, meaning that the device is systematically capable of meeting SIL 3 only when the proper hardware-fault tolerance and PFD_{avg} are also met for the SIF (including all devices in the entire loop, combined). To verify a SIL, the following needs to be considered:

- Systematic integrity (all elements need to have a systematic capability (SC) of 3 for a SIL 3 loop)
- Random integrity (PFD_{avg})
- Architectural constraints (hardware-fault tolerance, or HFT)

It is important to also note that the higher the SIL target, the more redundancy is typically required.

Misconception: Using an industry-leading SIL verification tool to select devices that meet the SIL target is sufficient for designing the SIF. Making the "numbers" (SIL verification) work is not a guarantee that the devices selected are appropriate for your process. Proper selection is required, and should consider process specifics, safety-function performance requirements and environmental conditions to safeguard against systematic failures from material incompatibility or undersized or misapplied hardware.

One relevant example focuses on the part of the SIF that generates the most failures. Statistically, the final element makes up 50% or more of the dangerous undetected failures in a SIF, as shown in Figure 5 [*1*]. In process applications, the logic solver and sensors are consistently self-testing and self-reporting — for example, a pressure transmitter takes measurements and reports them to the logic solver, which analyzes the measurements and decides whether to engage the final element. Meanwhile, the final element is typically in low demand. Thus, it remains in one position for most of its installed life until activated to perform its safety function. The final element also is in

TABLE 1: SAFETY INTEGRITY LEVELS WITH ASSOCIATED PFD_{AVG} AND RRF

Safety integrity level (SIL)	Average probability of failure (PFD_{avg}), low-demand mode of operation	Risk reduction factor (RRF; $1/PFD_{avg}$)
SIL 4	$\geq 10^{-5}$ to $<10^{-4}$	100,000 to 10,000
SIL 3	$\geq 10^{-4}$ to $<10^{-3}$	10,000 to 1,000
SIL 2	$\geq 10^{-3}$ to $<10^{-2}$	1,000 to 100
SIL 1	$\geq 10^{-2}$ to $<10^{-1}$	100 to 10

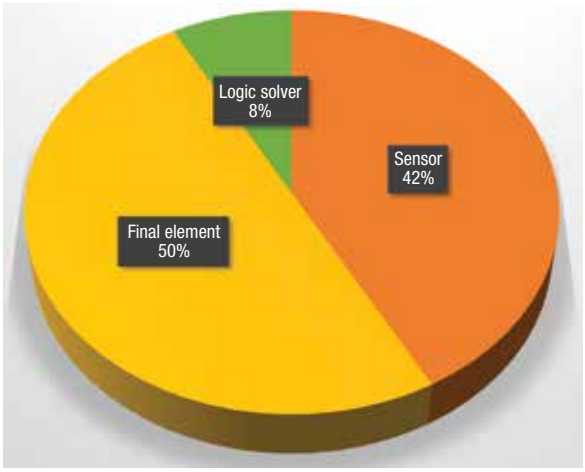

FIGURE 5. Final elements are the largest contributor to unplanned safety-system failures [*1*]

contact with the process fluid, making it susceptible to buildup within the valve and, thus, potentially unable to respond to a demand. This underlines the importance of not only properly testing the final element to ensure operation, but also makes the proper sizing, selection and engineering critical to meeting the safety function.

Misconception: If the SIL target is met in the initial design, it is good forever. Actually, proper testing of the SIF is required periodically to uncover dangerous undetected failure modes and maintain the SIL through the deemed operating lifetime (mission time). Once the SIF is installed, the equipment follows the normal bathtub-shaped reliability curve, which has a constant failure rate during its useful life. Thus, the SIL capability degrades over time in a predictable manner. To maintain the SIL required, the SIF must be tested periodically to prove that it can meet the safety function when called upon. These tests are called "proof tests" and are intended to identify dangerous undetected failure modes that are not otherwise detectable under normal process conditions through the mission time of the SIF.

Proof tests may include visual inspection, as well as performance testing, to meet safety-function specifics. For a final element, this commonly includes sending a trip signal from the logic solver and performing a full stroke from its normal to safe position, as well as verifying the stroke time. If tight shutoff is required, shutoff and leak rates would be tested. Devices and final elements that utilize diagnostics may be used to uncover additional degradation not otherwise apparent by visual inspection, such as the implementation of digital valve controllers on final elements to detect an increase in torque.

Performing proof testing often requires taking a device out of service. This can impact availability of operations. For the final element, a bypass can potentially be installed around the final element to enable proof testing without impacting operations. However, in some cases, space restrictions or installation cost with large line sizes makes installing a bypass more prohibitive. To maintain a SIL throughout the mission time, a partial stroke test is an option to supplement proof tests. Partial stroke tests can be performed in service while the process is running, stroking the final element over a portion of its total travel. This exercises the valve and proves that it can break out from its normal position, detecting a portion of the dangerous undetected failure modes of the final element. This test can be used to safely extend the proof-test interval or to meet required SIL with existing test intervals.

Although systems are usually complex, making it impossible in practice to fully determine every potential failure, proof testing is nevertheless essential to rule out as many options as possible and meet the SIL target through the mission time.

While SIS concepts and standards are becoming more well-recognized in the CPI, misconceptions still remain. Improved awareness and proper action will help to avoid associated systematic failures and to ensure a safer facility. ■

Edited by Mary Page Bailey

Reference

1. DNV GL A/S, Offshore Reliability Database (Oreda) Handbook, 2015.

Author

Afton Coleman is the senior marketing manager at Emerson for Fisher Digital Isolation Solutions (205 S. Center St., Marshalltown, IA 50158; Phone: +1-641-754-3439; Email: afton.coleman@emerson.com). She leads a product management team that works on the development of complete SIS final-element solutions. Coleman has supported functional safety and process application needs for multiple process industries, as well as the nuclear power industry, for over 14 years in her different roles with Emerson. She is a Certified Functional Safety Professional (CFSP). Coleman has a B.S.Ch.E. from the University of Iowa and an M.B.A. from Iowa State University.

Economic Indicators

2017 2018 2019

Download the CEPCI two weeks sooner at www.chemengonline.com/pci

CHEMICAL ENGINEERING PLANT COST INDEX (CEPCI)

(1957–59 = 100)	Oct. '19 Prelim.	Sept. '19 Final	Oct. '18 Final
CE Index	599.5	603.6	616.3
Equipment	727.6	733.7	751.5
Heat exchangers & tanks	627.8	637.0	666.9
Process machinery	721.7	723.5	728.3
Pipe, valves & fittings	958.4	960.6	982.8
Process instruments	420.5	422.8	419.7
Pumps & compressors	1072.3	1073.5	1038.0
Electrical equipment	560.8	561.8	552.6
Structural supports & misc.	771.7	785.9	830.6
Construction labor	338.4	338.4	340.4
Buildings	589.7	592.3	601.2
Engineering & supervision	314.4	314.0	316.6

Annual Index:
2011 = 585.7
2012 = 584.6
2013 = 567.3
2014 = 576.1
2015 = 556.8
2016 = 541.7
2017 = 567.5
2018 = 603.1

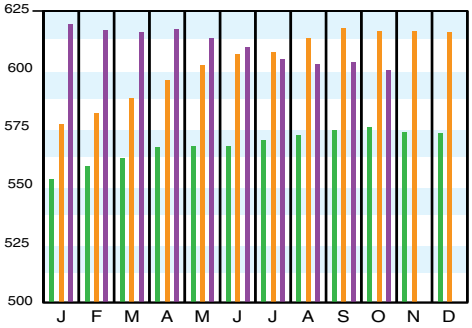

Starting in April 2007, several data series for labor and compressors were converted to accommodate series IDs discontinued by the U.S. Bureau of Labor Statistics (BLS). Starting in March 2018, the data series for chemical industry special machinery was replaced because the series was discontinued by BLS (see *Chem. Eng.*, April 2018, p. 76–77.)

CURRENT BUSINESS INDICATORS

	LATEST	PREVIOUS		YEAR AGO
CPI output index (2012 = 100)	Nov. '19 = 101.8	Oct. '19 = 101.7	Sept. '19 = 102.3	Nov. '18 = 104.2
CPI value of output, $ billions	Oct. '19 = 1,964.8	Sept. '19 = 1,963.6	Aug. '19 = 1,964.3	Oct. '18 = 2,023.0
CPI operating rate, %	Nov. '19 = 75.6	Oct. '19 = 75.6	Sept. '19 = 76.2	Nov. '18 = 78.4
Producer prices, industrial chemicals (1982 = 100)	Nov. '19 = 245.7	Oct. '19 = 249.5	Sept. '19 = 239.8	Nov. '18 = 277.6
Industrial Production in Manufacturing (2012 =100)*	Nov. '19 = 104.9	Oct. '19 = 103.8	Sept. '19 = 104.5	Nov. '18 = 105.8
Hourly earnings index, chemical & allied products (1992 = 100)	Nov. '19 = 187.0	Oct. '19 = 187.6	Sept. '19 = 184.6	Nov. '18 = 187.3
Productivity index, chemicals & allied products (1992 = 100)	Nov. '19 = 94.8	Oct. '19 = 94.7	Sept. '19 = 96.0	Nov. '18 = 97.9

CPI OUTPUT INDEX (2000 = 100)†

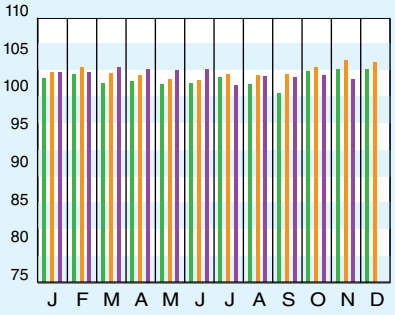

CPI OUTPUT VALUE ($ BILLIONS)

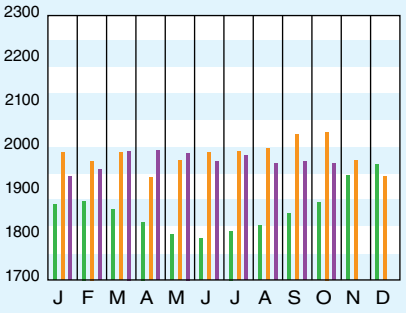

CPI OPERATING RATE (%)

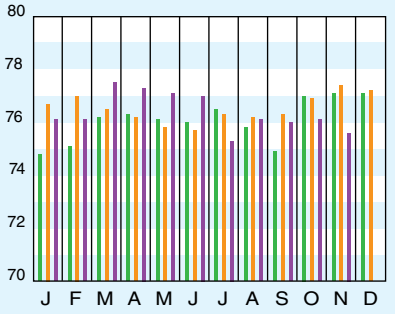

*Due to discontinuance, the Index of Industrial Activity has been replaced by the Industrial Production in Manufacturing index from the U.S. Federal Reserve Board.
†For the current month's CPI output index values, the base year was changed from 2000 to 2012
Current business indicators provided by Global Insight, Inc., Lexington, Mass.

CURRENT TRENDS

The preliminary value for the *CE* Plant Cost Index (CEPCI; top; the most recent available) for October 2019 decreased from the previous month's value, the seventh decline in the last nine months. The decrease in the overall CEPCI was driven by contractions in the Equipment and Buildings subindices. The Construction Labor subindex was flat, while the Engineering & Supervision subindex increased by a small margin. The final value for the previous month's CEPCI (September) was upwardly revised because of adjustments to the Process Control and Instruments Labor component of the CEPCI. The current CEPCI value is 2.7% lower than the corresponding value from a year ago at the same time.